2014

Integrated Robust Optimal Design (IROD) via sensitivity minimization

Punit Tulpule
Iowa State University

Integrated Robust Optimal Design (IROD) via sensitivity minimization

by

Punit J. Tulpule

A dissertation submitted to the graduate faculty

in partial fulfillment of the requirements for the degree of

DOCTOR OF PHILOSOPHY

Major: Mechanical Engineering

Program of Study Committee:

Atul Kelkar, Major Professor

Greg Luecke

Abhijit Chandra

Brian Steward

Umesh Vaidya

Iowa State University

Ames, Iowa

2014

TABLE OF CONTENTS

LIST OF TABLES

LIST OF FIGURES

ACKNOWLEDGEMENTS

I would like to take this opportunity to express my thanks to those who helped me with various aspects of conducting research and the writing of this thesis. First and foremost, Prof Atul Kelkar, my major professor, for his guidance, patience and support throughout this research and the writing of this thesis. His insights and words of encouragement have often inspired me and renewed my hopes for completing my doctorate degree. Besides my major professor I would like to thank all my committee members. I would also like to acknowledge John Deere for sponsoring this project, and specifically Todd Velde for fruitful discussions. I would additionally like to thank my brother, Dr Pinak Tulpule, for supporting, and inspiring me towards my career goals. I would also like to thank my parents and wife for encouraging me to pursue and complete my graduate studies.

ABSTRACT

A novel Integrated Robust Optimal Design (IROD) methodology is presented in this work which combines a traditional sensitivity theory with relatively new advancements in Bilinear Matrix Inequality (BMI) constrained optimization problems. IROD provides the least conservative approach for robust control synthesis. The proposed methodology is demonstrated using numerical examples of integrated control-structure design problem for combine harvester header and excavator linkages. The IROD methodology is compared with the state of the art sequential design method using the two application examples, and the results show that the proposed methodology provides a viable alternative for robust controller synthesis and often times offers even a better performance than competing methods. Although this method requires linearization of nonlinear system at each system parameter optimization step, a technique to linearized Differential Algebraic Equations (DAE) is presented which allows use of symbolic approach for linearization. This technique avoids repetitive linearizations. For the nonlinear systems with parametric uncertainties which can not be linearized at operating points, a new methodology is proposed for robust feedback linearization using sensitivity dynamics-based formulation. The feedback linearization approach is used for systems with augmented sensitivity dynamics and used to refine control input to improve robustness. The method is demonstrated using an example of a position tracking control of a hydraulic actuator. The robustness of controller design is demonstrated by considering variations in fluid density parameter. The results show that the proposed methodology improves robustness of the feedback linearization to parametric variations.

CHAPTER 1. OVERVIEW

The research presented in this thesis is focused on dynamical system-controller design methodology for linear systems and a robust feedback linearization of a class of nonlinear systems. Robustness of the closed loop system to variations in system parameters, is characterized by the sensitivity with respect to the parameter. With recent advancements in symbolic computation and automatic differentiation of complex equations, it is now possible to derive analytical expression for sensitivity dynamics. Expressing robustness in the form of sensitivity provides least conservative design, and it also facilitates automation of robust control synthesis process. This allows extension to integrated design of system and controller. It has been shown in the literature that integrated design provides better overall design as compared to sequential design method. The work in this thesis presents a methodology for Integrated Robut Optimal Design (IROD) of linear systems using Bilinear Matrix Inequalities(BMI). This methodology is then demonstrated by application to the integrated design of combine harvester header control system and excavator bucket level control. In many cases, for example multibody dynamics, the equations of motion (EOM) can be expressed in the form of differential algebraic equations (DAE). Hence, an alternative to linearization of differential algebraic equations (DAE) in symbolic form along with sensitivity dynamics is presented. Sensitivity-based robust design method for linear system is extended to include a class of nonlinear systems which are feedback linearizable with minimum phase zero dynamics.

1.1 Integrated Design

Traditionally, design of controlled mechanical systems is carried out in the sequential paradigm; that is, systems' all structural elements are first designed to meet certain functionality and strength criteria, and then the control design is accomplished to achieve some optimal controller performance. In such process, although the design is optimized at each step, overall design tends to be sub-optimal since the design space (or freedom) available at each step in the sequential process is smaller. On the contrary, in the integrated design paradigm, both structural (or mechanical) design and control design is accomplished concurrently on a much larger design space. The fact that even for linear systems with system parameter appearing linearly in the dynamical equations, the integrated design process is NP hard, makes the process challenging. An integrated design paradigm has been a topic of research since early 1980s. Some noteworthy research on integrated design includes work done under space station project for the design of controlled flexible space structures under Control-Structure Interaction (CSI) program at NASA in late 80's to early 90's. [1–4]. $\mathcal{H}_\infty$and $\mathcal{H}_2$ norm bound objective functions were minimized using integrated design approach in [5–8]. Variety of strategies are discussed in existing literature on simultaneous control/structure design. Optimization problems were solved using decomposition strategies in [9], and multistage optimization methods were used in [10]. The integrated design methods were employed for design of mechanical systems in [11] where a recursive experimental method using rapid prototyping was proposed. In [12], the concept of design for control was used for four bar mechanical linkage design. These researches do not consider robustness aspect of the design. Some early works in integrated robust design methodology for minimum sensitivity, variability and maximizing tolerance was proposed and demonstrated in [13, 14].

1.2 Robust Design Via Sensitivity Minimization

The robust optimal control problems were initially considered as the sensitivity minimal design problems until the beginnings of modern robust control theory. The sensitivity theory can be dated as back as 1945 when Bode in his famous book *Network analysis and feedback amplifier design* [15] defined sensitivity of performance with respect to an infinitesimal change in design parameter. The sensitivity theory was introduced in the textbooks [16], [17] in early 1960s. Many researchers [18], [19] and [20] and others in late 1960s considered trajectory sensitivity minimization problems by augmenting the sensitivity dynamics to the system dynamics. These researches were focused on LQR control problems, and the solution strategies were some variants of the maximum principle. Until the modern robust control theory based on uncertainty characterization was established, the sensitivity theory was the primary area of interest in robust control research. There is a large body of literature available in this area from the 1970s [21–25]. After the introduction to parametrization of all stabilizing controllers by Youla [26], and then $\mathcal{H}_\infty$optimal control by Zames et al. [27] sensitivity theory took a backstage.

Although the uncertainty based techniques are powerful and provide robust design over a range of uncertain parameters, the design is more conservative as the designer has to choose an upper bound on uncertainty. Also, it requires designers' skill deriving upper bound on uncertainty models, and expressing the uncertainty in form of additive, multiplicative or polytopic uncertainty. In the case of complex dynamical systems, uncertainty models may not be readily available. Hence, in [13, 14], the sensitivity minimization approach was considered for the robust optimal tracking of multi-body system which avoids estimation of uncertainty bounds on the part of designer. The recent advancements in the symbolic computation, and automatic differentiation further motivates the use of sensitivity-based integrated design methodology. In [13, 14], the sensitivity equations were directly computed by differentiating the equations of motion with respect to the

uncertain parameters. These articles also include a methodology wherein robust integrated design is achieved for optimal tolerancing in addition to tracking performance and optimal control. Subsequently, an alternative algorithm for sensitivity minimal robust optimal control was recently presented for linear systems using Youla parameterization in [28].

In third chapter of this thesis, the sensitivity theory and integrated design approach are combined with recent developments in Linear Matrix Inequality (LMI) to propose a new methodology for integrated locally optimal robust design. This new method preserves the benefits of sensitivity theory and uses relatively modern LMI methods to provide faster convergence.

1.3 Linear Matrix Inequalities (LMI)

LMI theory allows use of convex optimization methods in robust control of linear systems. Most of the robust optimal control design problems for linear systems, can be converted into a convex optimization problem by adding some conservatism. The initial research in LMI is well documented in [29], and recent research on the use of LMI theory in control systems with some applications is compiled in [30]. The LMI and Bilinear Matrix Inequalities (BMI) have been widely used in sub-optimal robust control design for last couple of decades. It is well known that the $\mathcal{H}_\infty$, $\mathcal{H}_2$ or mixed robust control design objectives for linear systems can be written in the form of BMI constrained optimization problems. Some of these problems can be converted into the equivalent LMI constrained problems by linearization change of variables [31], [32], or methods based on projection lemma [33]. These LMI constrained convex optimization problems are computationally easy to solve and many efficient algorithms have been developed. There are off the shelf software available, like Matlab robust control toolbox, which provide an efficient solution tool for LMI problems. Unfortunately, most of the

robust optimal control problems do not have equivalent LMI relaxations. Even though, the change of variables converts non-convex constraints into convex constrains, it adds conservatism. Hence, significant amount of research has been done on numerical approaches for BMI constrained optimization problems. The BMI constrained problems are generally NP-hard, but still, BMI relaxations and some heuristics provide polynomial time solution strategies. In literature, two types of solutions strategies namely, global optimization and local optimization can be found. The global optimization strategies are generally branch and bound algorithms [34], [35]. The global optimization algorithms suffer from computational issues and they are not polynomial time. Local optimal algorithms usually fix one variable of the BMI and solve the resulting LMI problem, then fix the other variable and solve the LMI problem, and iterate until the optimal solution is found. Obviously, the local search methods do not guarantee global minimum, and the resulting minimum depend on the initial conditions. The other iterative algorithm, the D-K iterations which iterate between control matrix K and scaling matrix D, is also not guaranteed to converge even at local minimum [36]. Although, the cone complementary linearization method [37] guarantees local optimal solution to the BMI constraint problem, it requires to solve an LMI problem at each step. Hence, in present research, a method proposed in [38] is modified to solve BMI constraint problems originating from sensitivity augmented systems. Specifically, the concept of using BMI constraint optimization presented in [38] is extended to solve the robust optimal control problem for sensitivity augmented linear systems. The theory presented in [38] needs to be modified since the sensitivity augmented system has special block lower triangular structure.

A sensitivity and performance norm minimization algorithm for full state feedback controller synthesis problem using LMIs was presented in [39]. In a parallel work [40], the authors have developed and demonstrated a BMI based algorithm for robust optimal controller synthesis via sensitivity augmented systems. It was shown that the algorithm is a viable alternative to uncertainty based $\mathcal{H}_\infty$or $\mathcal{H}_2$ or mixed controller design

techniques. The combination of LMI theory with sensitivity minimization of outputs preserves all the benefits of sensitivity theory but also makes use of modern convex optimization techniques of solving BMI problems emerging from the $\mathcal{H}_\infty$norm minimization. Use of sensitivity theory also keeps the number of complicating variables small as compared to polytopic uncertainty based robust synthesis. In this article, the approach of robust design is extended to integrated robust design where structure and control are designed concurrently. A two-step methodology is proposed inspired from existing BMI constrained optimization algorithm. The sensitivity theory facilitates automatic and less conservative computation of robustness, which allows evaluation of objective function in a loop. The method is presented for $\mathcal{H}_\infty$objective functions, but it can be easily extended to other objectives like $\mathcal{H}_2$ or mixed performance, or general quadratic performance.

1.4 Linearization of Multibody Dynamics

In order to use the IROD method for multibody dynamics, it is first necessary to linearize the EOM at operating point and derive linear sensitivity equations. The derivation of sensitivity equations requires differentiation with respect to the uncertain parameters. The multibody dynamical equations could get so large, that the symbolic representation can overload computer memory. These equations can be represented in form of DAE. Linearization of DAE requires solving the algebraic part, which is not possible in symbolic form, hence a method based on coordinate partitioning is developed. Early approaches for linearization of DAE were numerical [41–43] which do not provide exact linearizations. Some linearization methods produce linear DAE, but for optimal control design a different approach is required [44]. A practical approach for linearization is proposed in [45] which is based on multibody constrained formulation and variational principle. A similar method for linearizing multibody DAE based on coordinate partitioning and variational principle is given in [46].

1.5 Application to Combine and Excavator

The method presented in this thesis is applied to the Combine harvester header tracking problem and excavator bucket level control design problem.

1.5.1 Combine Header Height Control

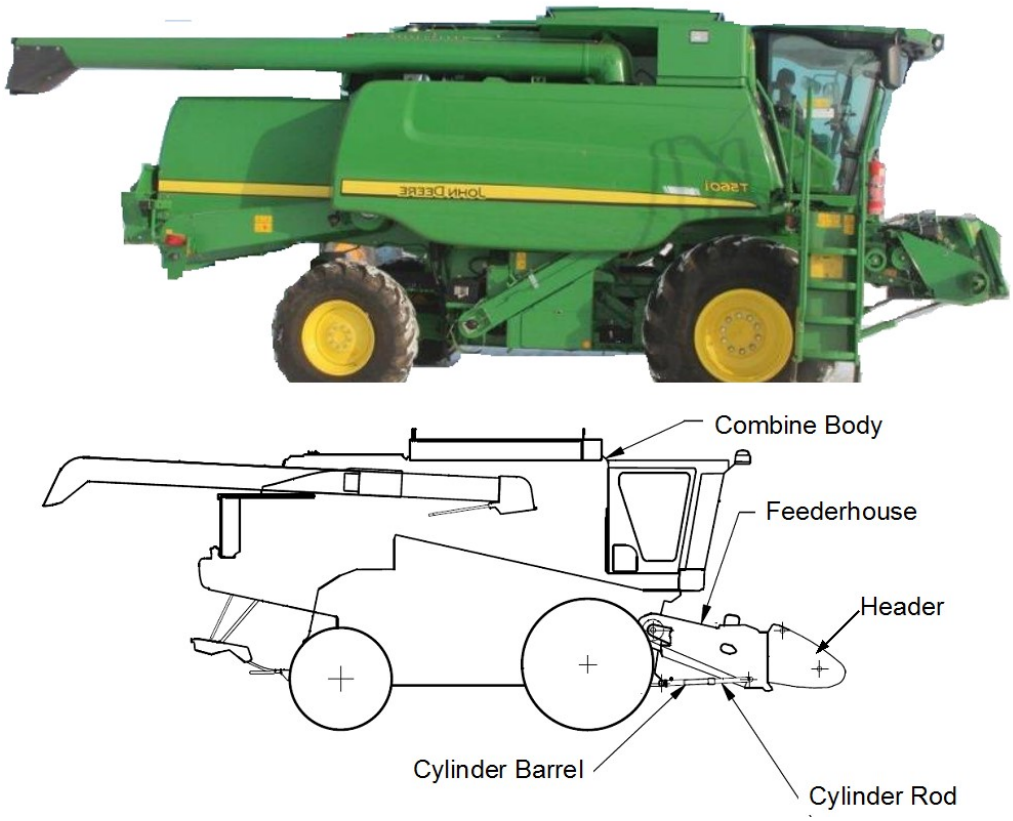

Figure 1.1 Picture and schematic diagram of combine harvester

A picture of combine harvester and associated schematic of combine harvester header linkage is shown in Fig. (1.1). The problem addressed is that of designing a mechanism and control system for a header linkage system that minimizes the control power, and at the same time maintains the prescribed height of of the header over rough terrain. The combine harvester has heavy header and the height needs to be automatically controlled for higher efficiency of harvest and speed of operation as the harvester moves over

rough terrain. The structure of this harvester imposes fundamental constraints on feedback control design [47]. A two DOF controller design using feed forward and feedback controller was presented in [48] and integrated plant/controller design based on only performance analysis was presented in [49] to overcome the bandwidth limitations due to the mechanical structure. In this research, a generalized methodology for Integrated and Robust Optimal Design (IROD) is applied to this example and it is shown that the new method provides better tracking, robustness, and minimizes control power than the state-of-the-art techniques such as robust $\mathcal{H}_\infty$design method.

1.5.2 Excavator Bucket Angle Control

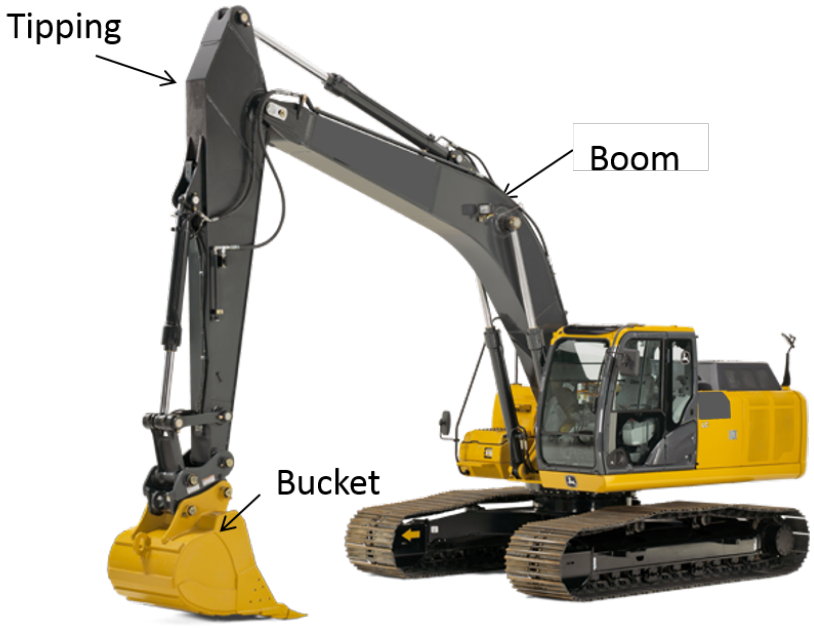

Figure 1.2 Picture of an excavator linkage

Another example presented is the design of robust control system for control of bucket angle in excavators. A picture of a representative excavator and a schematic of mechanism controlling bucket motion is shown in Fig. (1.2). The objective is to keep the bucket horizontal, to avoid spillover, while the operator moves the boom. A design variable is optimized for tracking error, sensitivity to variations in the mass of bucket and control

power. The challenge in this problem is to design controller which is robust to variations in the mass of the bucket, since load in the bucket is different in every operation. Results obtained using IROD method are compared with the results obtained from the state of the art robust control design method - polytopic uncertainty based $\mathcal{H}_\infty$control synthesis using LMI approach. Previous research on excavator control is mainly focused on automation of the entire excavator operation, which includes landscape shape sensing and path determination [50–52], but these studies did not include robust or integrated design. A robust $\mathcal{H}_\infty$controller for wheel loader bucket tracking was designed in [53], which included hydraulic actuator dynamics, but this research did not consider integrated design. For the wheel loader system, an integrated design approach was demonstrated in [54].

1.6 Robust Feedback Linearization

The method explained in the third chapter of this theses is applicable to only those systems which can be linearized at a given operating point. But there is a large class of nonlinear systems where determining a set of sensible operating points is not possible. For example, in case of hydraulic actuators determining a practical operating point outside the dead band is not possible. In classical nonlinear system control theory, variety of ways are available to design nonlinear controller for such systems. Feedback linearization has been very popular in nonlinear systems control because of its ability to control systems with most types of nonlinearities [55, 56] . Although feedback lienarization does not guarantee internal stability [57], depending on the zero dynamics, the method can locally design controllers for challenging nonlinear systems, such as example hydraulic actuators. While feedback linearization is good for tracking performance, it is known for not being robust to parametric uncertainties. The effectiveness of this method depends on the degree of accuracy of the system model. Robust stability of feedback linearization approach was addressed using Lyapunov design in earlier research, [58, 59]. In these ap-

proaches the uncertainty was assumed to be norm bounded which requires knowledge of the bounds as well as it adds conservativeness in the design. Robust feedback linearization for systems with parametric uncertainties were explained using high gain observers in [60], where set of integrators was obtained using nonlinear observer. Other approach towards robust feedback linearization is via Sliding Mode Control(SMC), [61, 62] which may provide discontinuous control input. Adaptive control is another widely used approach for robust nonlinear control design. A good compilation of earlier researches is available in [63]. Recently, a large body of research is concentrated on robustification of feedback linearization using techniques based on artificial neural networks or fuzzy logic. A brief literature review is available in a recently published research [64]. Uncertainty and disturbance estimation based approach is proposed in [65].

In this research, an alternative to existing robust feedback linearization approaches is proposed using sensitivity theory. This method provides the least conservative design since it does not require uncertainty estimate. This paper revisits the sensitivity theory along with feedback linearization to propose a new method for robustification by augmenting the sensitivity dynamics. The sensitivity information is used to update the control input for robust performance.

The proposed method is demonstrated using an example of linear plant model actuated with hydraulic actuator. Hydraulic systems are known to be very difficult to control, since there are dead bands, square root, and polynomial nonlinearities. H_∞ control design using polytopic uncertainty for excavator model including hydraulic actuator was presented in [53]. Mixed H_2 and H_∞ control design problem for earth moving equipment hydraulic power train was addressed in [66]. Feedback linearization and backstepping control design methods were implemented by many researchers for hydraulic actuators, some examples are - [67–70] but these researches did not include robustness considerations. The robust backstepping design for hydraulic system was proposed in [71]. Current research uses the proposed sensitivity-base methodology for robust feedback linearization

for hydraulic system consisting of a linear plant model actuated with a double acting cylinder with four way spool valve. The objective of this case study is to minimize the sensitivity of the closed loop system to variations in fluid density.

This thesis is outlined as follows- chapter 2 provides an efficient methodology to linearize generalized DAE using symbolic computation, chapter 3 gives the algorithm for IROD of linear systems. Results obtained from applications of IROD to combine harvester header height control problem and excavator bucket level control problem are presented in chapter 4. Chapter 5 explains a novel methodology for robust feedback linearization using sensitivity augmented nonlinear systems, and finally, thesis conclusions with future prospects of this research are discussed in chapter 6.

CHAPTER 2. LINEARIZATION OF MULTIBODY DYNAMICS IN SYMBOLIC FORM

In order to synthesize controller, and optimize system parameters simultaneously for nonlinear system using the method provided in chapter 3, the system dynamics needs to be linearized at operating point. One challenge is that the operating point changes as the design variable changes and hence the new linearization is needed. In the case of integrated design methods, the parameter is changed at each step in the parameter optimization loop, and optimal controller is found at each step. This method requires repetitive linearization of nonlinear systems. The process of linearization at each step can be reduced to a single one-time linearization if the linear system can be obtained as a function of design variable. With recent advancements in symbolic computation, it is feasible to differentiate equations in analytic form and keep functions in symbolic form. But, specifically for multibody systems, finding operating point and linearization as a function of design variable, may not be trivial due to equation swelling and large matrix inversions. There are various methods to derive EOM of multibody dynamics, which can be broadly classified into two groups, Newton's method and Lagrange method. Newton's method generally suffer from equation swelling, which means the equations could get very large. Lagrange equations generally provide DAE instead of ODEs, but this method can handle systems with large number of constraints and bodies. The DAE can be linearized at operating point to give linear DAE, but then the optimal control design requires additional theory. Hence, an efficient way of finding operating point and linearization of DAEs arising from multibody constraint formulation [72] is proposed in this chapter.

2.1 Multibody Constrained Formulation

Consider a planar multibody system with n of bodies and m constraint equations. This system has $3n - m$ degrees of freedom (DoF). Let the position states of multibody dynamics be $q = \begin{bmatrix} q_1 & q_2 & q_3 & \dots & q_{3\times n} \end{bmatrix}^T$ in a non inertial frame of reference, and let the constraint equations be $\phi(q,t) = 0$ where $\phi : \Re^{3\times n} \rightarrow \Re^m$ is a continuous function. Position states include X and Y coordinates of the CG of each body and angle of each body centered coordinate systems with respect to global coordinate system.

Notation: In this chapter, full derivatives are represented by subscript. For example, $\frac{d\phi}{dq}$ is written as ϕ_q.

For an unconstrained system of bodies the equations of motion are -

$$M\ddot{q} = Q \tag{2.1}$$

where, $M_{(3n\times 3n)}$ is the mass matrix and $Q_{(3n\times 1)}$ is the vector of external forces.

For constrained multibody dynamics, the constrained forces can be added to the EOM using Lagrange multipliers.

$$M\ddot{q} + \phi_q^T \lambda = Q \tag{2.2}$$

where $\lambda \in \Re^m$ is a vector of Lagrange multipliers. This vector equation has $3n + m$ unknowns ($3n$ states and m Lagrange multipliers) and only $3n$ linearly independent equations. Other m equations can be obtained by differentiating the constraints equations twice -

$$\begin{aligned} \phi &= 0 \\ \Rightarrow \dot{\phi} &= \frac{\partial \phi}{\partial t} + \phi_q \dot{q} = 0 \\ \Rightarrow \ddot{\phi} &= \phi_q \ddot{q} - \gamma = 0 \end{aligned} \tag{2.3}$$

Eq. (2.2) and Eq. (2.3) can be combined together to get DAE with $3n$ number of second order differential equations and m number of algebraic equations -

$$\begin{bmatrix} M & \phi_q^T \\ \phi_q & 0 \end{bmatrix} \begin{bmatrix} \ddot{q} \\ \lambda \end{bmatrix} = \begin{bmatrix} Q \\ \gamma \end{bmatrix} \tag{2.4}$$

2.2 Linearization

In order to linearize the differential algebraic equations, lets first solve for λ.

From equation Eq. (2.2)

$$\ddot{q} = M^{-1}Q + M^{-1}\Phi_q^T\lambda \tag{2.5}$$

Substitute for $\ddot{q}$ in Eq. (2.3).

$$\ddot{\Phi} = \Phi_q M^{-1}Q + \Phi_q M^{-1}\Phi_q^T\lambda - \gamma = 0 \tag{2.6}$$

$$\Rightarrow \lambda = -(\Phi_q M^{-1}\Phi_q^T)^{-1}\Phi_q M^{-1}Q + (\Phi_q M^{-1}\Phi_q^T)^{-1}\gamma \tag{2.7}$$

Now, substitute λ in Eq. (2.5).

$$\ddot{q} = M^{-1}Q + M^{-1}\Phi_q^T(\Phi_q M^{-1}\Phi_q^T)^{-1}\gamma - M^{-1}\Phi_q^T(\Phi_q M^{-1}\Phi_q^T)^{-1}\Phi_q M^{-1}Q \tag{2.8}$$

Equation (2.8) is a set of $3n$ second order differential equations. These equations can be linearized at operating point by finding jacobian with respect to q, but the resulting linear system has $6n$ states although the DOF of the system is $3n-m$. We expect that the minimal realization of resulting linear system should be of order $2(3n-m)$, because there are $2(3n-m)$ independent states and rest $2m$ states are dependent due to position and velocity constraint equations. The expected order of linear system can be achieved by minimal realization, but in practice minimal realization may not remove all dependent

states. This is because, Eq. (2.8) requires inverses of large matrices. This may add numerical issues depending on matrix condition numbers. Hence this method may not give desirable results. In order to get the linear model with order equal to $2(3n-m)$, the nonlinear system needs to be partitioned into dependent and independent coordinates. Next section explains linearization of multibody constrained equations using coordinate partitioning [44].

2.3 Coordinate Partitioning

The equation of motion obtained from virtual work is given in [44] -

$$\delta q^T (M\ddot{q} - Q) = 0 \tag{2.9}$$

The vector δq is virtual displacement in the system coordinates. The coefficient of virtual displacements can not be set to zero here, because the coordinates are not independent due to constraint equations. It can be assumed that all the constraint equations in ϕ are linearly independent, otherwise the dependent constraints can be removed to get a set of linearly independent constraint equations.

For virtual displacement in coordinates -

$$\phi_q \delta q = 0 \tag{2.10}$$

Since not all coordinates are independent, the state vector (system coordinates) can be partitioned as -

$$q = \begin{bmatrix} q_d^T & q_i^T \end{bmatrix}^T \tag{2.11}$$

where, q_d are m dependent states and q_i are $3n-m$ independent states. Hence from Eq. (2.10) -

$$\begin{aligned} \phi_{q_d}\delta q_d + \phi_{q_i}\delta q_i &= 0 \\ \Rightarrow \delta q_d &= -\phi_{q_d}^{-1}\phi_{q_i}\delta q_i \\ \delta q_d &= \phi_{di}\delta q_i \end{aligned} \tag{2.12}$$

$$\tag{2.13}$$

where, $\phi_{di} = -\phi_{q_d}^{-1}\phi_{q_i}$. The matrix ϕ_{q_d} is always invertible because the constraints are linearly independent. From the partitioning, the system coordinates can be written in form of virtual displacement of independent coordinates as -

$$\delta q = \begin{bmatrix} \delta q_d \\ \delta q_i \end{bmatrix} = \begin{bmatrix} \phi_{di} \\ I \end{bmatrix} \delta q_i = B_i \delta q_i \tag{2.14}$$

Now substituting for δq in Eq. (2.9), and since q_i are independent,

$$B_i^T(M\ddot{q} - Q) = 0 \tag{2.15}$$

Similarly, from Eq. (2.3),

$$\begin{aligned} \ddot{q}_d &= \phi_{di}\ddot{q}_i - \phi_{q_d}^{-1}\gamma \\ \ddot{q}_d &= \phi_{di}\ddot{q}_i + \phi_d \\ \Rightarrow \ddot{q} &= \begin{bmatrix} \phi_{di} \\ I \end{bmatrix} \ddot{q}_i + \begin{bmatrix} \phi_d \\ 0 \end{bmatrix} \\ &= B_i\ddot{q}_i + \gamma_i \end{aligned} \tag{2.16}$$

where, $\phi_d = \phi_{q_d}^{-1}\gamma$.

Now, substituting for $\ddot{q}$ in Eq. (2.15)

$$B_i^T M B_i \ddot{q}_i - B_i^T Q + B_i^T M \gamma_i = 0 \tag{2.17}$$

which can be written as -

$$\begin{aligned} \bar{M}_i \ddot{q}_i &= \bar{Q}_i \\ \ddot{q}_i &= \bar{M}_i(q_i, q_d)^{-1} \bar{Q}_i(q_i, q_d) \end{aligned} \tag{2.18}$$

where, $\bar{M}$ is a $(3n-m) \times (3n-m)$ mass matrix associated with independent states. and $\bar{Q}_i$ is generalized external force vector associated with independent states.

Equation 2.18 along with constraint equations $\phi(q_i, q_d) = 0$ give system of DAE, where there are $3n-m$ number of second order differential equations and m constraint equations. This can be written as $2(3n-m)$ first order differential equations, and $2m$ constraint equations by adding $\dot{\phi} = 0$ into constraint equations, i.e. the multibody dynamics EOM can be written in standard form of DAE as -

$$\begin{aligned} \mathcal{M}(q) \begin{bmatrix} \dot{q}_i \\ \dot{q}_{2_i} \end{bmatrix} &= \mathcal{Q}(q) \\ \Phi(q) &= 0 \end{aligned} \tag{2.19}$$

where, in case of multibody dynamics: $\mathcal{Q}(q) = \begin{bmatrix} q_{2_i}^T & \bar{Q}^T \end{bmatrix}^T$, $\Phi = \begin{bmatrix} \phi^T & \dot{\phi}^T \end{bmatrix}^T$, and

$$\mathcal{M} = \begin{bmatrix} I & 0 \\ 0 & \bar{M} \end{bmatrix} \tag{2.20}$$

where, I is a $3n \times 3n$ identity matrix. This Eq. (2.19) needs to be linearized at operating point. A generalized process to linearized DAE is proposed in next section.

2.4 Linearization of DAE

Let us express the DAE in general form as -

$$\begin{aligned} \mathcal{M}(x)\dot{x}_i &= \mathcal{Q}(x,u) \\ \Phi(x) &= 0 \end{aligned} \tag{2.21}$$

where, $x \in \Re^{\eta}$ are the states of the system, $\Phi : \Re^{\eta} \rightarrow \Re^{\eta_d}$ are the constraints, u is the external control input, $x_i \in \Re^{\eta_i}$ are the independent states, and $x_d \in \Re^{\eta_d}$ are dependent states, where $\eta_i + \eta_d = \eta$. Let the operating point of the system be $x = x_0$, where $\dot{x}|_{x_0} = 0$. Assume that $\mathcal{M}$ is invertible at operating point $x = x_0$. Now, x can be partitioned as $x = \begin{bmatrix} x_i^T & x_d^T \end{bmatrix}^T$. The linear system, from differential part of the DAE, can be written as -

$$\delta\dot{x}_i = A\delta x_i + B\delta u \tag{2.22}$$

where,

$$\begin{aligned} A &= \left[\frac{\partial \mathcal{M}^{-1}Q}{\partial x_i} + \frac{\partial \mathcal{M}^{-1}Q}{\partial x_d}\frac{\partial x_d}{\partial x_i}\right]\Bigg|_{x=x_0,u=u_0} \\ B &= \left.\frac{\partial \mathcal{M}^{-1}Q}{\partial u}\right|_{x=x_0,u=u_0} \end{aligned} \tag{2.23}$$

Now, $\frac{\partial x_d}{\partial x_i}$ can be obtained from the constraint equations. From the principle of variations we have-

$$\begin{aligned} \delta x^T \Phi_x &= 0 \\ \delta x_i^T \Phi_{x_i} + \delta x_d^T \Phi_{x_d} &= 0 \end{aligned} \tag{2.24}$$

$$\tag{2.25}$$

which, after taking limits as $\delta x_d \rightarrow 0$ and $\delta x_i \rightarrow 0$, implies

$$\frac{\partial x_d}{\partial x_i} = -\Phi_{x_d}^{-1}\Phi_{x_i} \tag{2.26}$$

The Φ_{x_d} matrix is always invertible since all the constraints can be assumed to be linearly independent.

Now the linear system is given by -

$$\begin{aligned} A &= \left[\frac{\partial \mathcal{M}^{-1}Q}{\partial x_i} + \frac{\partial \mathcal{M}^{-1}Q}{\partial x_d}\left(-\Phi_{x_d}^{-1}\Phi_{x_i}\right)\right]\Bigg|_{x=x_0,u=u_0} \\ B &= \left.\frac{\partial \mathcal{M}^{-1}Q}{\partial u}\right|_{x=x_0,u=u_0} \end{aligned} \tag{2.27}$$

The advantage of this method is that, the resulting linear system has η_i number of states, in other words, the resulting system has minimal realization. Also, this method requires finding only one inverse of $\mathcal{M}$. With advancements in symbolic computation, the derivatives can be computed in symbolic form. In some cases, for example multibody dynamics, $\mathcal{M}$ may not be inverted in symbolic form without computational overload. The computational problem can be avoided by a simple mathematical manipulation using the following identity -

$$(\mathcal{M}^{-1})_x\big|_{x=x_0} = -\mathcal{M}_x|_{x=x_0}\left(\mathcal{M}|_{x=x_0}\right)^{-1}\mathcal{M}_x|_{x=x_0} \tag{2.28}$$

In above equation, the right hand side does not have derivative of inverse. That means, now we do not require to find inverse of $\mathcal{M}$ in symbolic form, instead, x can be substituted by x_0 and then inverse can be found in numerical form. This eliminates the need of inverting large matrices in symbolic form. Hence combining Eq. (2.27) with the numerical trick Eq. (2.28) gives a way to linearize the nonlinear DAE at operating point using symbolic differentiation, without overloading memory. For integrated design, where a system parameter, for example mass or a link length, is to be designed concurrently with controller parameters, the parameter can be kept in symbolic form. In this case, $\mathcal{M}$ remains symbolic, but since has only a few symbolic variables it is still possible to invert $\mathcal{M}$ without computational overload. If a parameter is kept in symbolic form, resulting linear system is a function of the parameter and hence repetitive linearizations

can be avoided. For integrated design, where a system parameter, for example mass or a link length, is to be designed concurrently with controller parameters, the parameter can be kept in symbolic form. In this case, $\mathcal{M}$ remains symbolic, but since has only a few symbolic variables it is still possible to invert $\mathcal{M}$ without computational overload. If a parameter is kept in symbolic form, resulting linear system is a function of the parameter and hence repetitive linearizations can be avoided. Next chapter focuses on robust control synthesis for linear systems with parametric uncertainties.

CHAPTER 3. SENSITIIVITY BASED IROD METHODOLOGY

In the previous chapter a method was proposed to linearize nonlinear DAE that can be used with symbolic programming tools, like SymbolicMath toolbox of Matlab. This method facilitates linearization of complex DAE, keeping uncertain parameters in symbolic form. In this chapter a new method for Integrated Robust Optimal Design (IROD) is proposed based on sensitivity minimization and Bilinear Matrix Inequalities(BMI). If the linear system is expressed as a function of design variable and uncertain variable, then sensitivity dynamics of the linear model is obtained by differentiating the model with respect to uncertain parameter.

3.1 Sensitivity Based Robust Control Synthesis

3.1.1 Introduction to Parametric Sensitivity

The knowledge of sensitivity behavior plays a key role in robust analysis and synthesis of control systems. For a continuous plant model, the parametric sensitivities can be obtained by differentiating the dynamical equations with respect to the variables representing uncertain parameters or parameters that are subject to change over operating envelope of the system. Here, the continuity is implied in both, the time and parameter arguments. Performance sensitivity of a dynamical system can be defined as a small change in the performance for an arbitrarily small change in the design parameter.

Consider a system represented by differential equations

$$\dot{x} = f(x, u, b, t) \tag{3.1}$$

From the definition, the sensitivity equations can be written as -

$$\frac{d\dot{x}}{db} = \frac{df}{db} = \frac{\partial f}{\partial b} + \frac{\partial f}{\partial x}\frac{\partial x}{\partial b} \tag{3.2}$$

If the function $f \in \mathcal{C}^2$ i.e. f is second-order continuous, then the order of derivatives with respect to time and parameter b can be interchanged due to Clairout's theorem [73] (which is also known as Schwarz's theorem) and Eq. (3.2) becomes,

$$\dot{x}_b(x, x_b, u, b, t) = \frac{\partial f}{\partial b} + \frac{\partial f}{\partial x}x_b \tag{3.3}$$

where, $x_b = \frac{dx}{db}$ is the sensitivity of the states x with respect to the parameter b. The plant dynamics in Eq. (3.1) can now be augmented with sensitivity dynamics in Eq. (3.3) and solved simultaneously to obtain the system states, x, and sensitivity states, x_b. As a special case, consider a linear system -

$$G(b) = \left[\begin{array}{c|cc} A(b) & B_1(b) & B_2(b) \\ \hline C_1(b) & D_{11}(b) & D_{12}(b) \\ C_2(b) & D_{21}(b) & 0 \end{array}\right] \tag{3.4}$$

where, b is a vector of parameters which are uncertain, or subject to change due to wear and tear. The order of the system is n and there are n_z number of exogenous outputs, n_w number of exogenous inputs, and n_y number of output channels and n_u number of input channels which are used in the feedback. We assume differentiability of system matrices with respect to the parameters b. Given the controller dynamics in state space form - $K(A_{c_{(n_c \times n_c)}}, B_{c_{(n_c \times n_y)}}, C_{c_{(n_u \times n_c)}}, D_{c_{(n_u \times n_y)}})$ the parameter dependent closed-loop system can is given by -

$$\begin{aligned}
\mathcal{A}(b)_{(n+n_c)\times(n+n_c)} &= \begin{bmatrix} A(b) + B_2(b)D_cC_2(b) & B_2(b)C_c \\ B_cC_2(b) & A_c \end{bmatrix} \\
\mathcal{B}(b)_{(n+n_c)\times(n_w)} &= \begin{bmatrix} B_1(b) + B_2(b)D_cD_{21}(b) \\ B_cD_{21}(b) \end{bmatrix} \\
\mathcal{C}(b)_{n_z\times(n+n_c)} &= \begin{bmatrix} C_1(b) + D_{12}(b)D_cC_2 & D_{12}(b)C_c \end{bmatrix} \\
\mathcal{D}(b)_{n_z\times n_w} &= D_{11}(b) + D_{12}(b)D_cD_{21}(b)
\end{aligned} \tag{3.5}$$

Differentiating the closed loop system in Eq. (3.5) with respect to parameter b gives closed-loop parameter sensitivity dynamics. The augmented closed-loop system with this sensitivity dynamics can be written as -

$$G_{sen} = \begin{aligned}
\begin{bmatrix} \dot{X} \\ \dot{X}_b \end{bmatrix} &= \overbrace{\begin{bmatrix} \mathcal{A} & 0 \\ d\mathcal{A}/db & \mathcal{A} \end{bmatrix}}^{\hat{\mathcal{A}}_{(2(n+n_c)\times 2(n+n_c))}} \begin{bmatrix} X \\ X_b \end{bmatrix} + \overbrace{\begin{bmatrix} \mathcal{B} \\ d\mathcal{B}/db \end{bmatrix}}^{\hat{\mathcal{B}}_{(2(n+n_c)\times n_w)}} w \\
\begin{bmatrix} z \\ z_b \end{bmatrix} &= \overbrace{\begin{bmatrix} \mathcal{C} & 0 \\ d\mathcal{C}/db & \mathcal{C} \end{bmatrix}}^{\hat{\mathcal{C}}_{(n_z\times 2(n+n_c))}} \begin{bmatrix} X \\ X_b \end{bmatrix} + \overbrace{\begin{bmatrix} \mathcal{D} \\ d\mathcal{D}/db \end{bmatrix}}^{\hat{\mathcal{D}}_{(n_z\times n_w)}} w
\end{aligned} \tag{3.6}$$

(The dependence of system matrices on parameter b is not explicitly written hereon, but it is assumed.) where, $X \in \Re^{n+n_c}$ is a vector of closed loop states with $X = [x; x_c]$, x_c being the controller states. X_b are the closed loop sensitivity states with $X_b = [x_b; x_{c_b}]$. Again subscript b indicates derivative w.r.t. b. Please note that -

- The matrix $\hat{\mathcal{A}}$ has block lower triangular structure, with the same blocks on diagonal. Hence, the augmented system has repeated Eigen values.
- The exogenous inputs of the system are parameter independent, hence derivative of input dw/db is zero.
- The two outputs of the system include the nominal system response and the sensitivity response of the system.

3.1.2 $\mathcal{H}_\infty$-Norm Bound Objective

If the objective is to find only the optimal controller that minimizes the $\mathcal{H}_\infty$norm bound of system in Eq. (3.6), then the constraint can be written as a BMI [29]

$$\begin{bmatrix} sym(P_1\hat{\mathcal{A}}) & P_1\hat{\mathcal{B}} & \hat{\mathcal{C}}^T \\ * & -\gamma I & \hat{\mathcal{D}}^T \\ * & * & -\gamma I \end{bmatrix} \prec 0 \tag{3.7}$$

where, $\begin{bmatrix} x; & x_c; & x_b; & x_{c_b} \end{bmatrix}^T P_1 \begin{bmatrix} x; & x_c; & x_b; & x_{c_b} \end{bmatrix}$ is the quadratic Lyapunov function for G_{sen} and γ is the $\mathcal{H}_\infty$norm bound to be minimized. The BMI constrained problem is written in standard optimization form as -

$$\begin{aligned} \underset{vec(A_c),vec(B_c),vec(C_c),vec(D_c),vec(P_1)}{\text{minimize}} \quad & \gamma \\ \text{subject to} \quad & (3.7), \\ & P_1 \succ 0 \end{aligned} \tag{3.8}$$

The BMI constrained optimization problem in Eq. (3.8) can not be equivalently converted into an LMI constrained problem using linearization change of variables or projection lemma. Linearization change of variables is done by doing a state transformation and then replacing all the nonlinear terms by new variables. The resulting constraint is an LMI in new variables. The LMI problem is then solved to obtain the optimal parameters. The actual design parameters can be obtaiend by inverse relation between the new variables and design variables. This requires a one-one and onto relationship between new and actual variables. In the case of problem in Eq. (3.8), the one-one and onto relation does not exist. Hence the linearization change of variables fails in this case. Next section explains why change of variable fails.

3.1.3 Linearization Change of Variables (Failed)

In order to solve the sensitivity based robust optimal control problem, we can try linearization of the BMI in Eq. (3.7) via change of variables.

For simplicity, lets assume that P_1 has block diagonal structure according to $\hat{\mathcal{A}}$ as -

$$P_1 = \begin{bmatrix} P & 0 \\ 0 & P \end{bmatrix}$$

This assumption adds conservatism, but this linearization fails even after adding conservatism.

Lets define P and Q as -

$$P = \begin{bmatrix} X & U \\ U^T & * \end{bmatrix} \text{ and, } P^{-1} = \begin{bmatrix} Y & V \\ V^T & * \end{bmatrix} \tag{3.9}$$

and

$$Q = \begin{bmatrix} Y & I \\ V^T & 0 \end{bmatrix} \quad Z = \begin{bmatrix} I & 0 \\ X & U \end{bmatrix} \tag{3.10}$$

Note here that $QP = Z$ and $XY + UV^T = I$.

With these definitions lets define the transformation on sensitivity augmented system G_{sen}.

$$\left[\begin{array}{cc|c} Q^T(P\mathcal{A})Q & 0 & Q^TP\mathcal{B} \\ Q^T(P\mathcal{A}_b)Q & Q^T(P\mathcal{A})Q & Q^TP\mathcal{B}_b \\ \hline \mathcal{C}Q & 0 & \mathcal{D} \\ \mathcal{C}_bQ & \mathcal{C}Q & \mathcal{D}_b \end{array}\right] \tag{3.11}$$

Note here that, in addition to the terms including nominal plant model, now there are additional terms which include derivatives of the plant model. From Eq. (3.7), the sensitivity augmented system -G_{sen} has $\mathcal{H}_\infty$norm less than γ iff $\exists P \succ 0$ such that

$$\begin{bmatrix} sym(Q^T(P\mathcal{A})Q) & Q^T(\mathcal{A}_b^T P)Q & Q^T P\mathcal{B} & Q\mathcal{C}^T & Q\mathcal{C}_b^T \\ * & sym(Q^T(P\mathcal{A})Q) & Q^T P\mathcal{B}_b & 0 & \mathcal{C}Q \\ * & * & -\gamma I & \mathcal{D}^T & \mathcal{D}_b \\ * & * & * & -\gamma I & 0 \\ * & * & * & 0 & -\gamma I \end{bmatrix} \prec 0 \tag{3.12}$$

Now, lets define K_b,L_b, M_b and N_b such that -

$$Q^T(P\mathcal{A}_b)Q = \begin{bmatrix} A_bY + B_bM + BM_b & A_b + B_bNC + BN_bC + BNC_b \\ K_b & X + L_bC + LC_b \end{bmatrix} \tag{3.13}$$

Using the change of variables in Eq. (3.13), the BMI in Eq. (3.12) can be transformed into an LMI, with controller decision parameters K,L, M, N, K_b,L_b, M_b, and N_b, and Lyapunov paramters X and Y. The control decision parameters are now 8, and *unfortunately there is no bijection from these parameters to control parameters* A_c, B_c, C_c, *and* Dc. The relationship between new parameters K_b,L_b, M_b, and N_b and actual control parameters is given by -

$$\begin{bmatrix} K_b & L_b \\ M_b & N_b \end{bmatrix} = \begin{bmatrix} XA_bY & 0 \\ 0 & 0 \end{bmatrix} + \begin{bmatrix} U & XB_{2_b} \\ 0 & I \end{bmatrix} \begin{bmatrix} A_c & B_c \\ C_c & D_c \end{bmatrix} \begin{bmatrix} V^T & 0 \\ C_{2_b}Y & I \end{bmatrix} \tag{3.14}$$

Also there is a bijection from the control parameters to K,L, M, N. -

$$\begin{bmatrix} K & L \\ M & N \end{bmatrix} = \begin{bmatrix} XAY & 0 \\ 0 & 0 \end{bmatrix} + \begin{bmatrix} U & XB_2 \\ 0 & I \end{bmatrix} \begin{bmatrix} A_c & B_c \\ C_c & D_c \end{bmatrix} \begin{bmatrix} V^T & 0 \\ C_2Y & I \end{bmatrix} \tag{3.15}$$

There is no constraint which guarantees that the controllers obtained from the relation Eq. (3.14) and Eq. (3.15) are same. Hence, the linearization of BMI has failed in this case. We did not get a unique controller from linearization of the BMI.

This requires to solve the BMI problem using numerical techniques.

The next section is a modification in the algorithm presented in [38] to solve BMI constrained problem arising from the sensitivity augmented systems.

3.2 Solution Strategy

The algorithm presented here gives a locally optimal solution to BMI constrained minimization problems.

3.2.1 Locally Optimal Robust Control Design

A general BMI can be written as -

$$\mathbb{M}(x,y) = F_{00} + \sum_{i=1}^{N_x} F_{i0}x_i + \sum_{j=1}^{N_y} F_{0j}y_j + \sum_{i=1}^{N_x}\sum_{j=1}^{N_y} F_{ij}x_i y_j \prec 0 \tag{3.16}$$

where $x \in \mathcal{R}^{N_x}$ and $y \in \mathcal{R}^{N_y}$ are the design variables, $\mathbb{M}$ is the BMI and F are the real matrices of dimension equal to the BMI. Also, $F_{ij} = F_{ij}^T \ \forall i,j$. Note here that the variables x or y includes the Lyapunov function, control parameters and the norm bound γ. The generalized BMI constrained robust optimal control problem can be written as -

$$\begin{aligned} & \min_{x,y,\gamma} \ \gamma \\ \text{such that} \quad & \mathbb{M}(x,y) \prec 0 \\ & \langle c,x\rangle + \langle d,y\rangle < \gamma \\ & \underline{x} \le x \le \overline{x}, \ \underline{y} \le y \le \overline{y} \end{aligned} \tag{3.17}$$

where, $\underline{(\cdot)}$ and $\overline{(\cdot)}$ represent the lower and upper bounds on the variable $(\cdot)$. The vectors c and d define the performance objective. This restriction comes from the technical details, which can be found in [38].

First, the feasibility problem with BMI in Eq. (3.16) is written as a optimization problem using the Frobenius norms and projection properties. Define a function for

fixed value of γ

$$\nu_\gamma(x,y) = \left\| [\mathbb{M}]^+ \right\|_F^2 \tag{3.18}$$

The projection of a symmetric matrix on positive definite matrix essentially keeps the positive eigenvalues and all the negative Eigen values are replaces negative eigen values with zeros. The Frobenius norm is square root of sum of singular values, hence it can be seen that ν is essentially a sum of all positive singular values. Therefore, if ν is zero then the BMI $\mathbb{M}$ is less than or equal to zero. Also, the converse is true i.e. if the $\mathbb{M} \prec 0$ is feasible then ν is zero. Hence,

$$\exists x,\ y \text{ s.t. } \mathbb{M} \prec 0 \Leftrightarrow \min_{x,y} \nu_\gamma(x,y) = 0 \tag{3.19}$$

In Eq. (3.19) we have converted the BMI feasibility problem into an optimization problem. The basic idea is to find the initial feasible solution of $\mathbb{M} \prec 0$ for some γ, then use bisection on γ to find the local minimum. Now consider a minimization problem -

$$\min_{x,y} \nu_\gamma(x,y) \tag{3.20}$$

The gradient of the objective function can be computed using a lemma that can be found in [38]. A cautious BFGS method, or quasi-Newton type methods can be used to solve the minimization problem in Eq. (3.20) with gradient derived in the lemma.

In order to start the bisection method to minimize γ, upper bound and lower bounds on γ need to be determined.

3.2.2 Lower Bound

The lower bound can be computed using the so-called relaxed LMI problem [34].

$$\begin{aligned} & \gamma_{LB} = \min_{x,y} \ \langle c, x\rangle + \langle d, y\rangle \\ \text{subject to} \quad & \underline{x} \le x \le \overline{x}, \ \underline{y} \le y \le \overline{y} \ \underline{w} \le w \le \overline{w} \\ & \mathbb{M}(x, y, w) \prec 0 \end{aligned} \tag{3.21}$$

where, $w_{ij} = x_i y_j$ and $\underline{w} = \min(\underline{x}\underline{y}, \overline{x}\underline{y}, \underline{x}\overline{y}, \overline{x}\overline{y})$ and $\overline{w} = \max(\underline{x}\underline{y}, \overline{x}\underline{y}, \underline{x}\overline{y}, \overline{x}\overline{y})$

If this problem is not feasible for any $\gamma \ge 0$, then the original problem in Eq. (3.17) is also not feasible, but the feasibility of this problem does not guarantee the feasibility of the original problem. In other words, lower bound may not be feasible.

3.2.3 Initial Robust Control Design (Upper Bound)

It is not trivial to find the initially feasible solution. In this sub section we demonstrate a way to find initially feasible solution. The initial feasible solution to the BMI of $\mathcal{H}_\infty$norm bound can be found by first finding the feasible solution for full state static gain feedback case, and then the output feedback case. Consider the plant model in Eq. (3.4) and controller model $K(A_c, B_c, C_c, D_c)$.

3.2.3.1 Static Gain Feedback

Consider a full state static gain feedback i.e. assume $K = F$. The closed loop system with full state static gain feedback is given by -

$$G_{cl}(\mathcal{A}_F, \mathcal{B}_F, \mathcal{C}_F, \mathcal{D}_F) = \left[\begin{array}{cc|c} A + B_2 F & 0 & B_1 \\ A_b + B_{2_b} F & A + B_2 F & B_{1_b} \\ \hline C_1 + D_{12} F & 0 & D_{11} \\ C_{1_b} + D_{12_b} F & C_1 + D_{12} F & D_{11_b} \end{array}\right] \tag{3.22}$$

The $\mathcal{H}_\infty$norm of the closed loop system, $\|G_{cl}\|_\infty < \gamma$, iff $\exists P_1 \succ 0$ such that the BMI in Eq. (3.23) is feasible.

$$\begin{bmatrix} sym(P_1\mathcal{A}_F) & P_1\mathcal{B}_F & \mathcal{C}_F^T \\ * & -\gamma I & \mathcal{D}_F^T \\ * & * & -\gamma I \end{bmatrix} \prec 0 \tag{3.23}$$

Note that P_1 is pre multiplied and F is post multiplied to B_2 in the term $P_1\mathcal{A}_F$. Hence, the change of variables is not helpful immediately. Let $Q_1 = {P_1}^{-1} \succ 0$. Transform G_{cl} using Q_1. The BMI in Eq. (3.23) becomes

$$\begin{bmatrix} sym(\mathcal{A}_F Q_1) & \mathcal{B}_F & Q_1\mathcal{C}_F^T \\ * & -\gamma I & \mathcal{D}_F^T \\ * & * & -\gamma I \end{bmatrix} \prec 0 \tag{3.24}$$

Partition $Q_1 = Q \oplus Q \oplus Q \oplus Q$ according to $\mathcal{A}_F$. Additional conservatism is added due to this assumption, but in this section we are finding only the feasible solution. Now parameterize the nonlinear terms - $FQ = L$. The change of variables converts the BMI in Eq. (3.24) into an LMI -

$$\begin{bmatrix} sym(\mathbb{A}) & \mathbb{B} & \mathbb{C}^T \\ * & -\gamma I & \mathbb{D}^T \\ * & * & -\gamma I \end{bmatrix} \prec 0 \tag{3.25}$$

where,

$$\mathbb{A} = \begin{bmatrix} AQ + B_2L & 0 \\ A_bQ + B_{2_b}L & AQ + B_2L \end{bmatrix} \quad \mathbb{B} = \begin{bmatrix} B_1 \\ B_{1_b} \end{bmatrix}$$

$$\mathbb{C} = \begin{bmatrix} C_1Q + D_{12}L & 0 \\ C_{1_b}Q + D_{12_b}L & C_1Q + D_{12}L \end{bmatrix} \quad \mathbb{D} = \begin{bmatrix} D_{11} \\ D_{11_b} \end{bmatrix}$$

The Eq. (3.25) is an LMI in L and Q. If the optimal control problem

$$\begin{aligned} \underset{L,Q}{\text{minimize}} \quad & \gamma \\ \text{subject to} \quad & (3.25) \\ & Q \succ 0 \end{aligned} \tag{3.26}$$

is solved to obtain the lowest norm bound γ_{min}, then no other controller can give better performance (i.e. γ) than γ_{min}. Knowing the static gain feedback controller, the output dynamic feedback controller can be determined by solving an LMI problem.

3.2.3.2 Dynamic Feedback

Now, fix $C_c = F$ and $D_c = 0$ in K. Consider an output feedback control -

The closed loop system G_{cl} is defined in Eq. (3.5). The control input for full state static gain feedback controller is $u_{static} = Fx$, and the control input for dynamic feedback controller is $u_{dynamic} = C_c x_c$. When $C_c = F$, the performance of dynamic output feedback controller will be comparable to the full state static gain feedback controller, if only if the controller states $x_c \to x$. When this is true, $u_{dynamic} \to u_{static}$. Similarly, the sensitivity output in first case will be similar to the second case only if $x_{c_b} \to x_b$. This leads to a change of states $\tilde{x} = x - x_c$ and $\tilde{x_b} = x_b - x_{c_b}$. Now define the linear transformation T such that $[x, \tilde{x}, x_b, \tilde{x_b}] = T[x, x_c, x_b, x_{c_b}]^T$.

$$T = \begin{bmatrix} I & 0 \\ I & -I \end{bmatrix} \oplus \begin{bmatrix} I & 0 \\ I & -I \end{bmatrix} \tag{3.27}$$

The closed loop system in Eq. (3.6) is transformed using matrix T.

$$\begin{bmatrix} \tilde{\mathcal{A}} & \tilde{\mathcal{B}} \\ \tilde{\mathcal{C}} & \tilde{\mathcal{D}} \end{bmatrix} = \begin{bmatrix} T\hat{\mathcal{A}}T & T\hat{\mathcal{B}} \\ \hat{\mathcal{C}}T & \hat{\mathcal{D}} \end{bmatrix} \tag{3.28}$$

The matrices $\tilde{\mathcal{A}}$ $\tilde{\mathcal{B}}$, $\tilde{\mathcal{C}}$ and $\tilde{\mathcal{D}}$ are obtained by Eq. (3.29)

$$\begin{bmatrix} \tilde{\mathcal{A}} & \tilde{\mathcal{B}} \\ \tilde{\mathcal{C}} & \tilde{\mathcal{D}} \end{bmatrix} =$$

$$\left[\begin{array}{cccc|c} A+B_2F & -B_2F & 0 & 0 & B_1 \\ A+B_2F-B_cC_2-A_c & A_c-B_2F & 0 & 0 & B_1-B_cD_{21} \\ A_b+B_{2_b}F & -B_{2_b}F & \diamond & \diamond & B_{1_b} \\ A_b+B_{2_b}F-B_cC_{2_b} & -B_{2_b}F & \diamond & \diamond & B_{1_b}-B_cD_{21_b} \\ \hline C_1+D_{11}F & -D_{11}F & 0 & 0 & D_{11} \\ C_{1_b}+D_{11_b}F & -D_{11_b}F & C_1+D_{11}F & -D_{11}F & D_{11_b} \end{array}\right] \tag{3.29}$$

where, $\diamond$ terms follow from the fact that $\tilde{\mathcal{A}}$ is lower block triangular and diagonal blocks are identical. The $\mathcal{H}_\infty$norm of the closed loop system, $\|G_{cl}\|_\infty < \gamma$, iff $\exists P_1 \succ 0$ such that the BMI in Eq. (3.30) is feasible.

$$\begin{bmatrix} sym(P_1\tilde{\mathcal{A}}) & P_1\tilde{\mathcal{B}} & \tilde{\mathcal{C}} \\ * & -\gamma I & \tilde{\mathcal{D}} \\ * & * & -\gamma I \end{bmatrix} \prec 0 \tag{3.30}$$

Now, partition $P_1 = P \oplus P_c \oplus P_b \oplus P_c \succ 0$ according to $\tilde{\mathcal{A}}$. Here, F is kept fixed and the only design variables are A_c, B_c and P, P_c, P_b. Combining the non linear terms the BMI in Eq. (3.30) can be transformed into an LMI.

$$\begin{bmatrix} sym(\mathbb{M}) & \mathbb{N} & \tilde{\mathcal{C}}^T \\ * & -\gamma I & \tilde{\mathcal{D}}^T \\ * & * & -\gamma I \end{bmatrix} \prec 0 \tag{3.31}$$

where $\mathbb{M}$ is shown in Eq. (3.32)

$$\mathbb{M} = P_1\tilde{\mathcal{A}} = \begin{bmatrix} P(A_F) & -PB_2F & 0 & 0 \\ P_c(A_F) - Z - GC_2 & Z - P_cB_2F & 0 & 0 \\ P_b(A_{Fb}) & -P_bB_{2_b}K & P_b(A_F) & -P_bB_2F \\ P_c(A_{Fb}) - GC_{2_b} & -P_cB_{2_b}F & P_c(A_F) - Z - GC_2 & Z - P_cB_2F \end{bmatrix} \tag{3.32}$$

where, $A_F = A + B_2F$ and $A_{Fb} = A_b + B_{2_b}F$.

$$\mathbb{N} = P_1\tilde{\mathcal{B}} = \begin{bmatrix} PB_1 \\ P_cB_1 - GD_{21} \\ PB_{1_b} \\ P_cB_{1_b} - GD_{21_b} \end{bmatrix}$$

where, $Z = P_cA_c$ and $G = P_cB_c$.

Note here that the parameters P, P_c, P_b, Z, and G appear affinely in the LMI (3.31). This LMI can be solved for $P_1 \succ 0$, Z and G. Then the control parameters A_c and B_c can be obtained. The control parameters, A_c, B_c, $C_c = F$ and $D_c = 0$ obtained from this LMI feasibility problem give a feasible solution which is considered as an upper bound (γ_{UB}) to the original BMI problem (3.7). This solution is treated as an initial feasible solution for starting the bisection.

3.3 Integrated Robust Sub-Optimal Design

In integrated design, both control parameters and structural parameters are optimized for performance in a single optimization problem. In the form of the equation, the integrated design problem can be written as-

$$\begin{aligned} \underset{b,vec(A_c),vec(B_c),vec(C_c),vec(D_c)}{\text{minimize}} \quad & \text{Performance function} \\ \text{subject to} \quad & \underline{b} \leq b \leq \bar{b} \end{aligned} \tag{3.33}$$

Note that the set of optimization variables include the vector of structural design parameters. The $\mathcal{H}_\infty$norm bound optimization problem in Eq. (3.8) can be extended to an integrated problem by adding the vector of structural parameters b into the optimization variables as-

$$\begin{aligned} \underset{vec(A_c),vec(B_c),vec(C_c),vec(D_c),vec(P_1),b}{\text{minimize}} \quad & \gamma \\ \text{subject to} \quad & (3.7), \\ & P_1 \succ 0 \\ & \underline{b} \leq b \leq \bar{b} \end{aligned} \tag{3.34}$$

In the integrated design problem settings, the matrix inequality in Eq. (3.7) is not a BMI because now it includes additional variable terms in b. In general, the integrated design problems can not be written as BMI constrained problem, therefore a two step algorithm for integrated design is proposed in this section.

3.3.1 Algorithm

This section summarizes the algorithm for integrated robust optimal design (IROD) methods to solve the problem in Eq. (3.33) using BMI method explained in section 3. The integrated design problem can be split into two nested optimization problems as -

$$\begin{aligned} \underset{b}{\text{minimize}} \quad & \gamma_{min} \\ \text{subject to} \quad & \left[\begin{array}{ll} \gamma_{min} = \underset{vec(A_c),vec(B_c),vec(C_c),vec(D_c),vec(P_1)}{\text{minimize}} & \gamma \\ \text{subject to} & (3.7), \\ & P_1 \succ 0 \end{array} \right] \\ & \underline{b} \leq b \leq \bar{b}, \end{aligned} \tag{3.35}$$

The algorithm to solve the inner problem is given below:

Define a vector of all decision variables $d = [vec(A_c), vec(B_c), vec(C_c), vec(D_c), vec(P_1), b]$. Then, the solution steps are:

1. *Step 1: Find the lower bound γ_{LB}^0 by solving problem in Eq. (3.21).*

2. *Step 2: Find upper bound* γ_{UB}^0 *and initially feasible variables* d^* *by first solving the full state static gain feedback control problem in Eq. (3.25) and then solving the output feedback control problem in Eq. (3.31).*

3. *Step 3: Set maximum number of iterations* N_{itr} *and allowed tolerance* Tol*. Set* $k = 0$

4. *Step 4: Compute new* γ *by bisection method,* $\gamma^{k+1} = (\gamma_{LB}^k + \gamma_{UB}^k)/2$*. Check the feasibility of* γ^{k+1} *by solving the BMI problem in Eq. (3.20). BFGS methods or quasi-Newton methods can be used to solve this problem to get locally optimal* $\nu_\gamma(d)$*.*

5. *Step 5: If* $\nu_\gamma(d) = 0$ *then the BMI is feasible for* γ^{k+1}*. Change the upper bound to* $\gamma_{UB}^{k+1} = \gamma^{k+1}$ *and keep the lower bound same* $\gamma_{LB}^{k+1} = \gamma_{LB}^k$*. Change* $d^* = d$*. If* $\nu_\gamma(d) > 0$ *then the BMI is not feasible for* γ^{k+1}*, then Change the lower bound to* $\gamma_{LB}^{k+1} = \gamma^{k+1}$ *and keep the upper bound same i.e.* $\gamma_{UB}^{k+1} = \gamma_{UB}^k$ *and keep the value of* d^* *same.*

6. *Step 6: If* $k = N_{itr}$ *or* $\gamma_{UB}^{k+1} - \gamma_{LB}^{k+1} \leq Tol$ *then the locally optimal value of* γ *is* γ^{k+1} *and the optimal decision variables are* d^**. Otherwise, go to Step 4.*

The outer problem can be solved using algorithms that guarantee local convergence; for example, interior point methods. Since, the algorithm used for solving BMI constrained problems guarantee local convergence, the integrated design is guaranteed to be locally optimal. In most cases the upper bound obtained by solving convex optimization problems in Eq. (3.25) and Eq. (3.31), is very close to the local minimum, hence in many practical cases, the bisection can be avoided and the upper bound can be assumed as the minimum. The algorithm of IROD is shown in Fig. (3.1)

Next chapter presents simulation results from application of this algorithm to Combine harvester header height control problem.

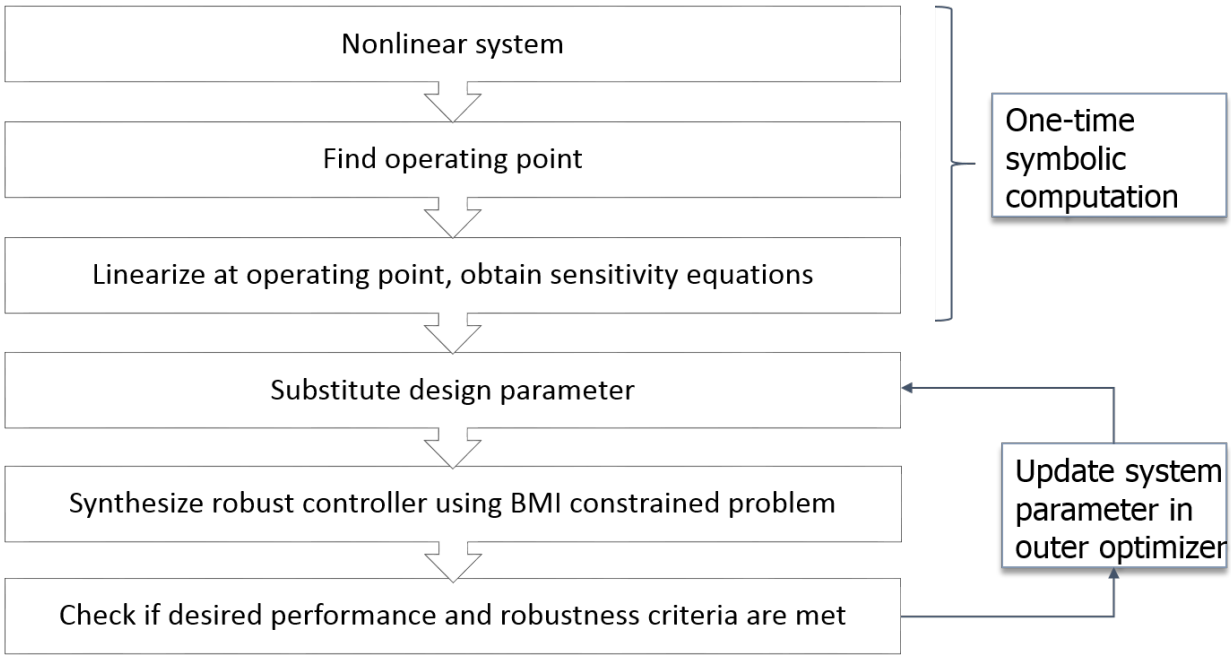

Figure 3.1 Algorithm of IROD

CHAPTER 4. APPLICATION TO COMBINE HARVESTER AND EXCAVATOR

4.1 Combine Harvester Header Height Control

IROD methodology proposed in the previous chapter is employed to simultaneously design controller and a mechanical linkage design parameter for header height tracking problem of combine harvester. The integrated design objective relates to an improved terrain tracking, which directly relates to increased productivity, and reduced control power, which directly translates to reduction in fuel costs. Also robust design allows reduced manufacturing costs and better performance for longer period of time. In the second section, the methodology is used to simultaneously design excavator link parameter and bucket level controller.

Schematic diagrams of combine machine and header link are shown in Fig. (4.1) and Fig. (4.2), respectively.

The objective of this case study is to synthesize a robust controller and optimize a header linkage parameter to maintain a constant header height above the sinusoidal terrain, minimize the sensitivity of performance with respect to changes in the same plant parameter and reduce control power. The plant design variable is chosen to be location of a pin joint (LB) between feeder house and hydraulic piston in body centered coordinate system as shown in Figure 4.2. Nominal value of LB is $1.541m$. The uncertain parameter was chosen to be LB because this parameter has wider range due to less physical constraints. The header height control problem is important because even

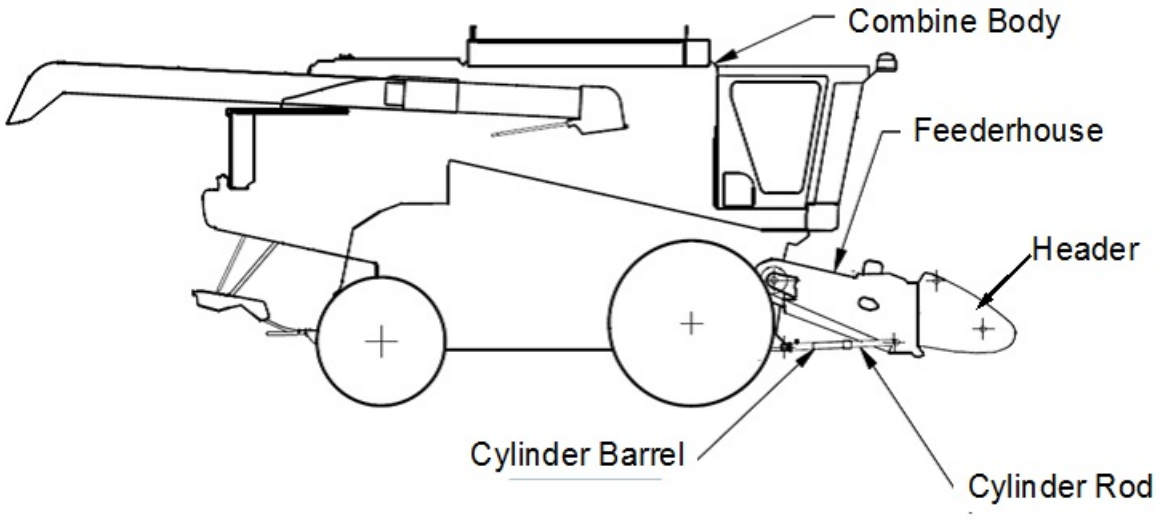

Figure 4.1 Schematic diagram of combine harvester

small improvement in tracking is directly related to higher crop harvest due to improved precision, better speed of combine harvester which then relates to leveraged profit for farmer. In this study, we assumed the speed of combine machine to be 10 mph (16.1 km/h) and designed two controllers using two methods namely, robust $\mathcal{H}_\infty$design using LMI and integrated robust optimal design (IROD) method. The plant parameter LB was re-designed using IROD method. The parameters of the linkage are for 9870STS combine machine of Deere and company. The rough terrain is the reference input for tracking (Input 1) and the header height is controlled through hydraulic actuator (Input 2). The hydraulic actuator is assumed as a perfect source of force. The four tires are modeled as a spring-mass-damper system. The height sensor is attached at the tip of the header, and there is a natural delay between header and front tires and rear tires. Velocity of the combine is assumed to be a constant at 10 mph ($4.4707 m/s$) and since the distance between the header height sensor and the tires is known, the delay between header height sensor and front tires is 0.5810s and the delay between header height sensor and rear tires is 1.37s. These delays are modeled using first order Pade approximation. The model of the header, feeder-house linkage along with the vehicle and tires is built

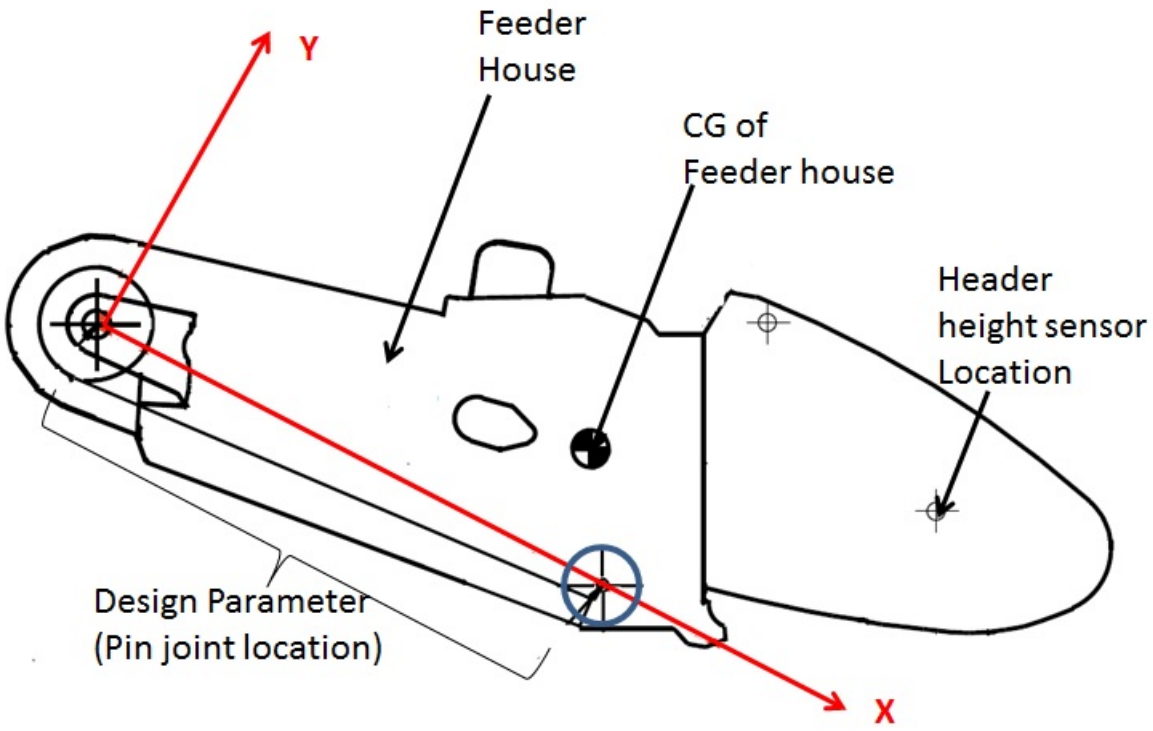

Figure 4.2 Schematic diagram of combine header

in SimMechanics. The dynamics incorporated in the SimMechanics model is shown in Fig. (4.3).

4.1.1 Sequential $\mathcal{H}_\infty$Design

In order to design robust $\mathcal{H}_\infty$optimal controller, parameter LB was varied in the range of $\pm 0.1m$ from nominal value with step size of $0.005m$. At every discrete value of LB,the harvester model was linearized to obtain a family of plant models with uncertainty in the parameter LB. Uncertainty in the model is modeled as polytopic uncertainty. Bode magnitude diagrams of normalized uncertain plants and upper bound on uncertainty are shown in Fig. (4.4).

Terrain tracking controller does not require high frequency tracking. The weighting function w_T on reference input is shown in Eq. (4.1).

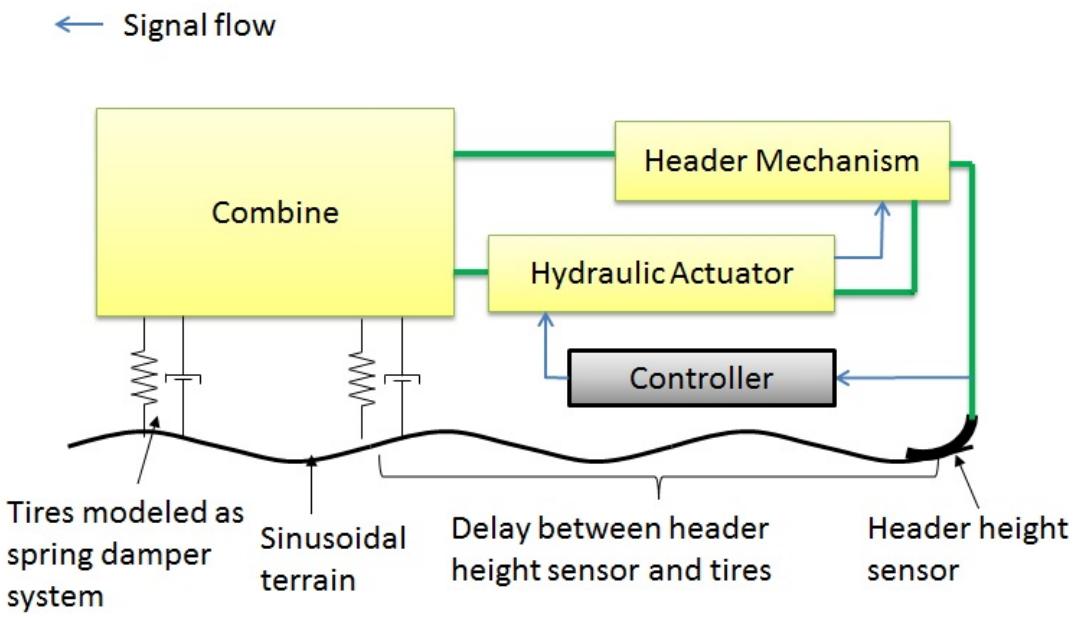

Figure 4.3 Schematic of the dynamics included in the system model

$$w_T = \frac{(s+10)}{(s+10000)} \tag{4.1}$$

$\mathcal{H}_\infty$optimal control is synthesized for the set of uncertain plant models uG using LMI method. Another controller without considering uncertainty was designed using the same method. For nominal controller,the same weighting function is used as shown in Eq. (4.1)

4.1.2 Integrated Robust Optimal Design (IROD)

The IROD theory is used to derive controller and system parameter LB such that the sensitivity w.r.t. the same parameter LB, the tracking error and control power are minimized. The SimMechanics model of combine harvester is linearized at operating point such that the header is raised to desired height. The linear sensitivity dynamics is obtained by numerical differentiation of linearized SimMechanics model. The minimum $\mathcal{H}_\infty$norm bound problem for the augmented system and sensitivity dynamics is solved

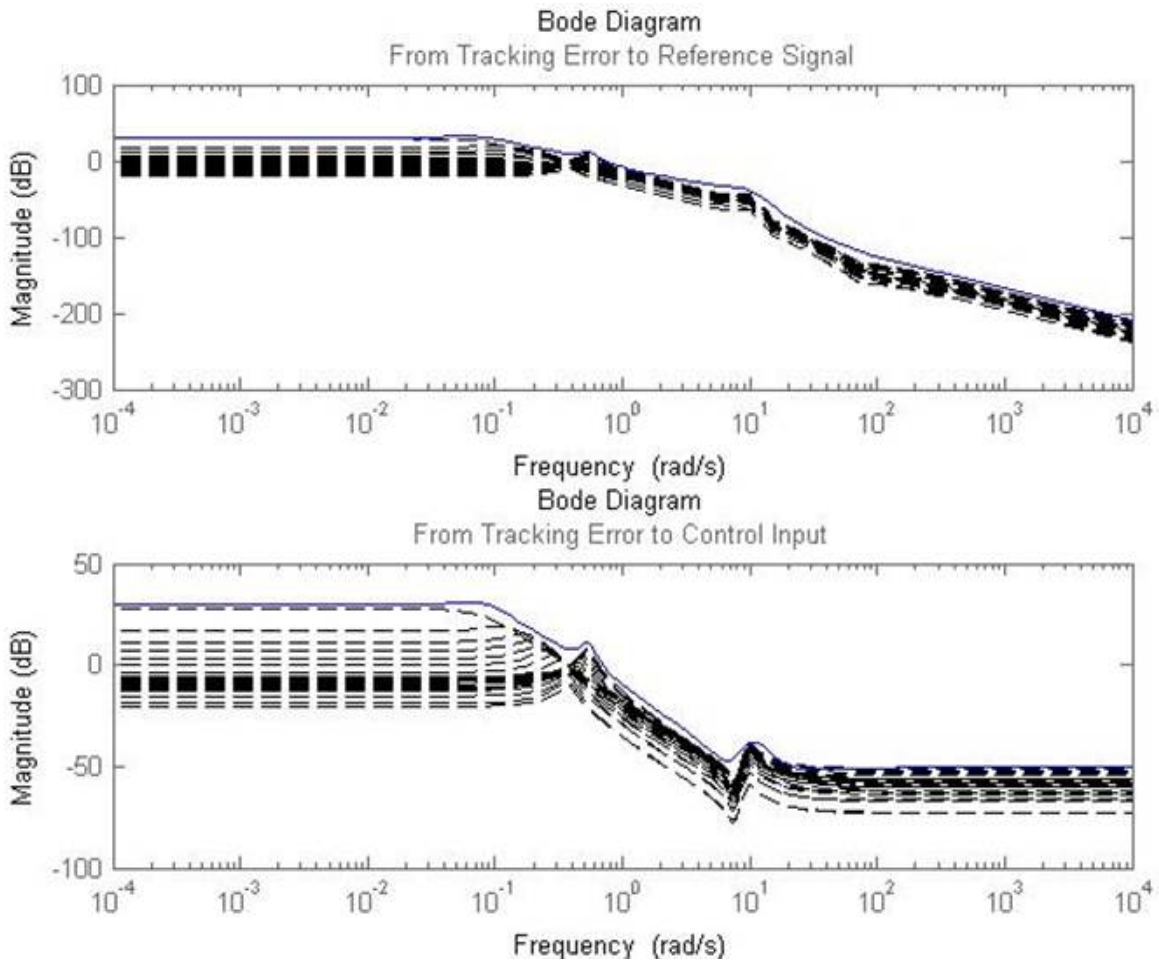

Figure 4.4 Set of normalized uncertain models: dashed black lines represent uncertain model and solid blue line represents the upper bound

using IROD method explained in the third chapter. The system is linearized at every step of the optimization since, when LB is changed, the operating point as well as linearization of nonlinear system changes. The IROD method proposed the piston joint location to be moved closer to the header pivot. The proposed change in the position is $\delta LB = -6.36cm$. Integrated design shows 14% improvement in $\mathcal{H}_\infty$norm from $\gamma_{nominal} = 11.64$ to $\gamma_{integrated} = 9.9123$.

Figure 4.5 shows comparison between performance of controller obtained from robust $\mathcal{H}_\infty$control synthesis and closed loop system obtained from IROD. All the three (nominal $\mathcal{H}_\infty$, robust $\mathcal{H}_\infty$and IROD) controllers are used in the loop with full nonlinear system

Table 4.1 Comparison between $\mathcal{H}_\infty$controller and IROD

	$\mathcal{H}_\infty$	Robust $\mathcal{H}_\infty$	Integrated Design
RMS Tracking Error (m)	0.144934	0.026668	0.008066
Maximum absolute sensitivity	1.1047	0.1543	0.0172
Total Control Power(J)	2.264×10^6	2.1167×10^6	1.9480×10^6

developed in SimMechanics. Terrain shape is chosen to be sinusoidal with amplitude $1m$ and frequency $0.1Hz$ ($0.2\pi rad/sec$) i.e. $0.1406rad/m$ and period $44.84m$, if combine velocity is $4.4707m/s$ ($10mi/hr$). The sensitivity of the closed loop system in all three cases is computed as a function of angle of header, using numerical differentiation. Figure 4.6 compares the maximum sensitivities of the closed loop systems obtained from different approaches. Table 4.1 shows that the integrated design method gave better results in terms of all the three design criteria. All the three measures (RMS error, control power, and sensitivity) are computed for steady state performance.

4.2 Excavator Bucket Level Control

In this study robust optimal control along with a link length are simultaneously designed for bucket angle control of an excavator. A diagram of a typical excavator is shown in Fig. (4.7). The design variable is the length of link (LB_e) indicated in the figure. While moving the load, bucket angle should be maintained such that the bucket angle is held constant with respect to ground to avoid any spilling of the load. An automatic controller is needed to control the bucket angle when an operator changes the angle of the boom. The challenge is to design a controller that is robust to the variations in mass of the bucket (MB), since the load in bucket is not known and changes in every operation. Other objective of the study is to minimize the control power required to maintain the level. All the parameters for excavator are taken from AMEsim excavator demo. The

hydraulic actuators are modeled as perfect sources of force. The nominal value of design variable is $1.45m$. Two methods are used to design controller, the robust $\mathcal{H}_\infty$design and IROD methodology explained in chapter 2 and chapter 3.

Equations of motion for the mechanical system are derived using method explained in chapter 2. The uncertain parameter MB and the design variable LB_e are kept as symbolic variables. The EOM are then linearized at an operating point, which also depends on MB and LB_e, using linearization algorithm explained in chapter 2. The linearized models are written in generalized linear model form with bucket angle tracking error, tipping control force, and bucket control force as exogenous outputs. The exogenous inputs are boom angle and tipping angle reference inputs. Control inputs are the tipping actuator force and bucket actuator force, and measured outputs are bucket angle and tipping angle.

4.2.1 Sequential and Integrated Design

An $\mathcal{H}_\infty$controller is designed for the nominal value of the design variable. The uncertainty in the mass of the bucket is modeled as polytopic uncertainty. The upper bound and lower bound on the mass is assumed $\pm 10\%$ of the nominal value. The uncertain mass range from lower bound to upper bound is linearly gridded by 10 points, and linear systems at all the grid points are obtained by substituting values in the symbolic linear systems. LMI based algorithm is used to find optimal controller. The IROD method is used to design another $\mathcal{H}_\infty$norm minimal controller, and design parameter LB_e which minimizes the sensitivity with respect to change in MB. Method explained in chapter 3 is used to design control variables and LB_e. Lower bound on the design variable is set to be $1.15m$ and the upper bound is set to $2.16m$ which is a constraint arising from the structure of the excavator. Output weighting function on the tracking error for both the design processes is taken as a low pass filter -

Table 4.2 Comparison between $\mathcal{H}_\infty$controller and IROD

	Robust $\mathcal{H}_\infty$	Integrated Design	% Improvement
RMS Tracking Error (rad)	1.406	1.289	8.32%
Maximum absolute sensitivity (rad/KG)	1.3095×10^{-4}	0.79443×10^{-4}	39.33%
Total Control Power(J)	9.2292×10^{5}	6.0449×10^{5}	34.5%

$$W_p(s) = \frac{s+1}{s+0.01} \tag{4.2}$$

The control force output is weighted by scalar function - $W_c = 10^{-5}$.

4.2.2 Results

IROD method proposed to increase LB_e to $1.97m$ for optimal performance. In order to compare the two designs, the boom angle is actuated using sinusoidal signal with frequency $1rad/s$, and amplitude $0.1rad$. Reference input for bucket angle is set to πrad to ensure the bucket remains parallel to ground, also the tipping reference angle is $0.6545rad$. The comparison between tracking error of sequential $\mathcal{H}_\infty$design and IROD are presented in Fig. (4.8). The control inputs, resulting from $\mathcal{H}_\infty$design and integrated design, to the bucket and tipping are shown in Fig. (4.9). Table 4.2 shows that the IROD methodology performs better than the state of the art control synthesis method in terms of all the three design objectives, i.e. performance, robustness and control power.

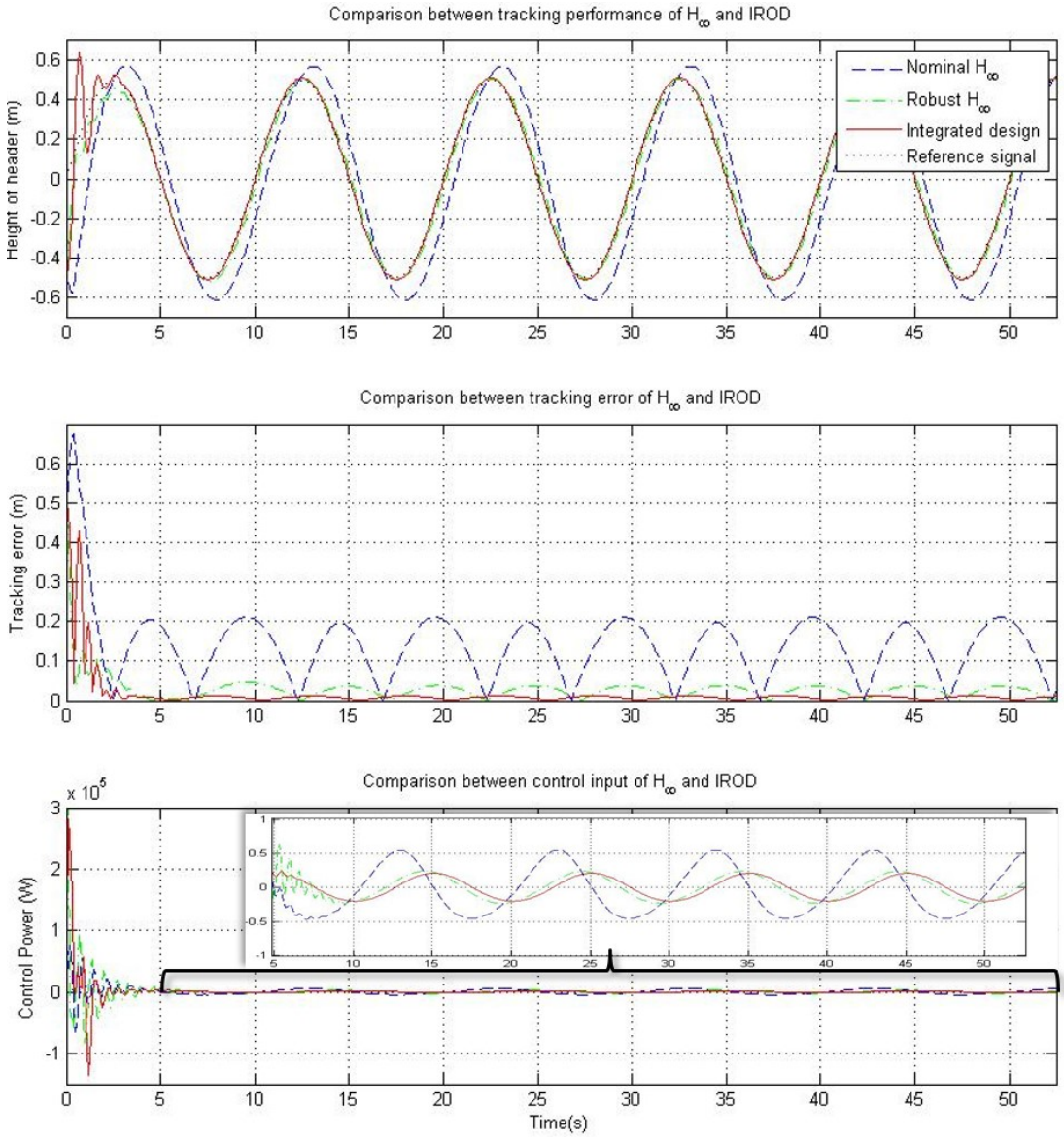

Figure 4.5 Comparison between tracking performance and control power of $\mathcal{H}_\infty$design and IROD

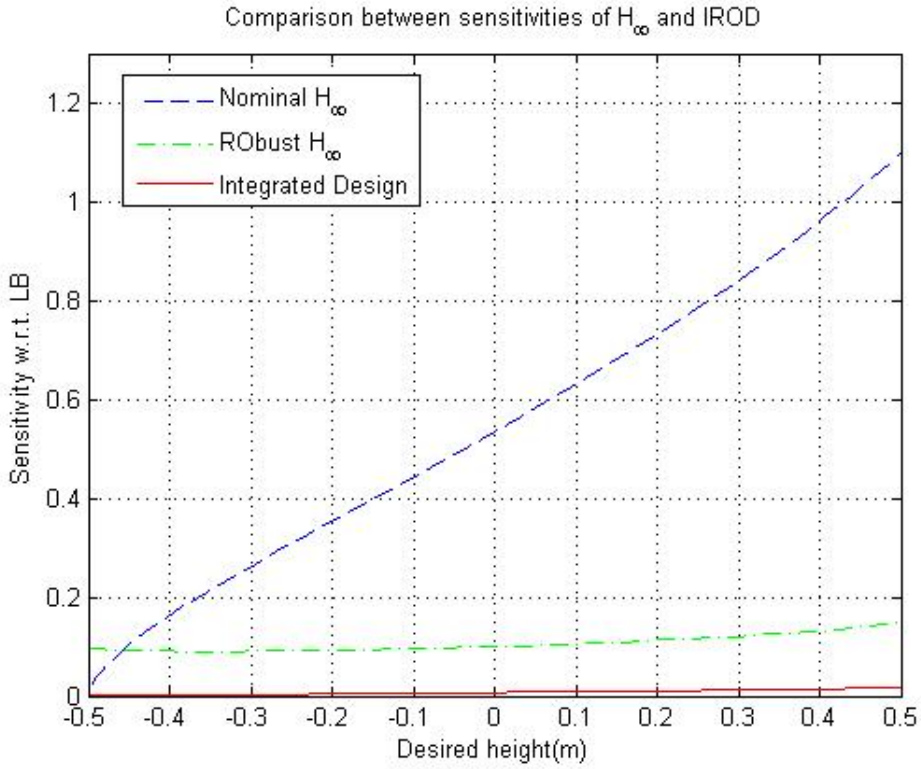

Figure 4.6 Comparison of sensitivities of performance as functions of header angle

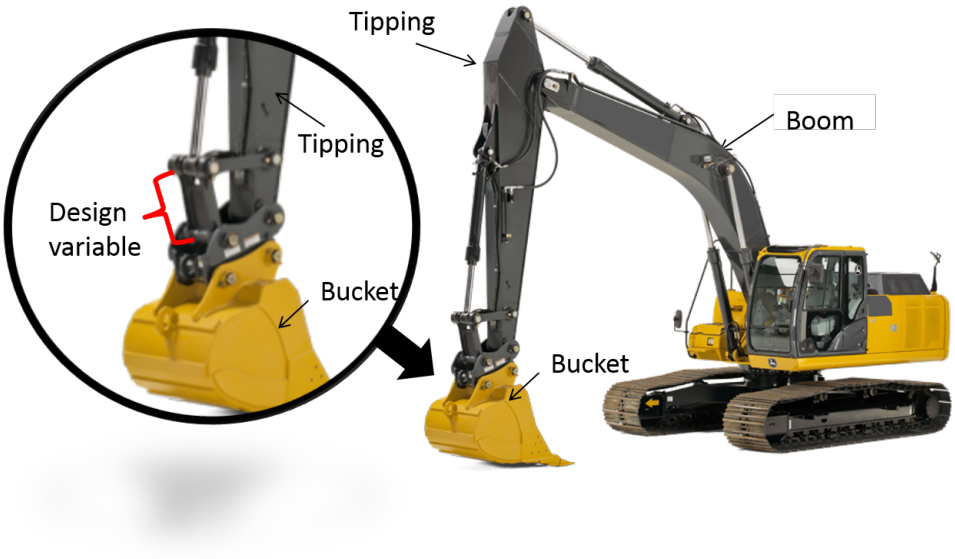

Figure 4.7 Schematic diagram of excavator

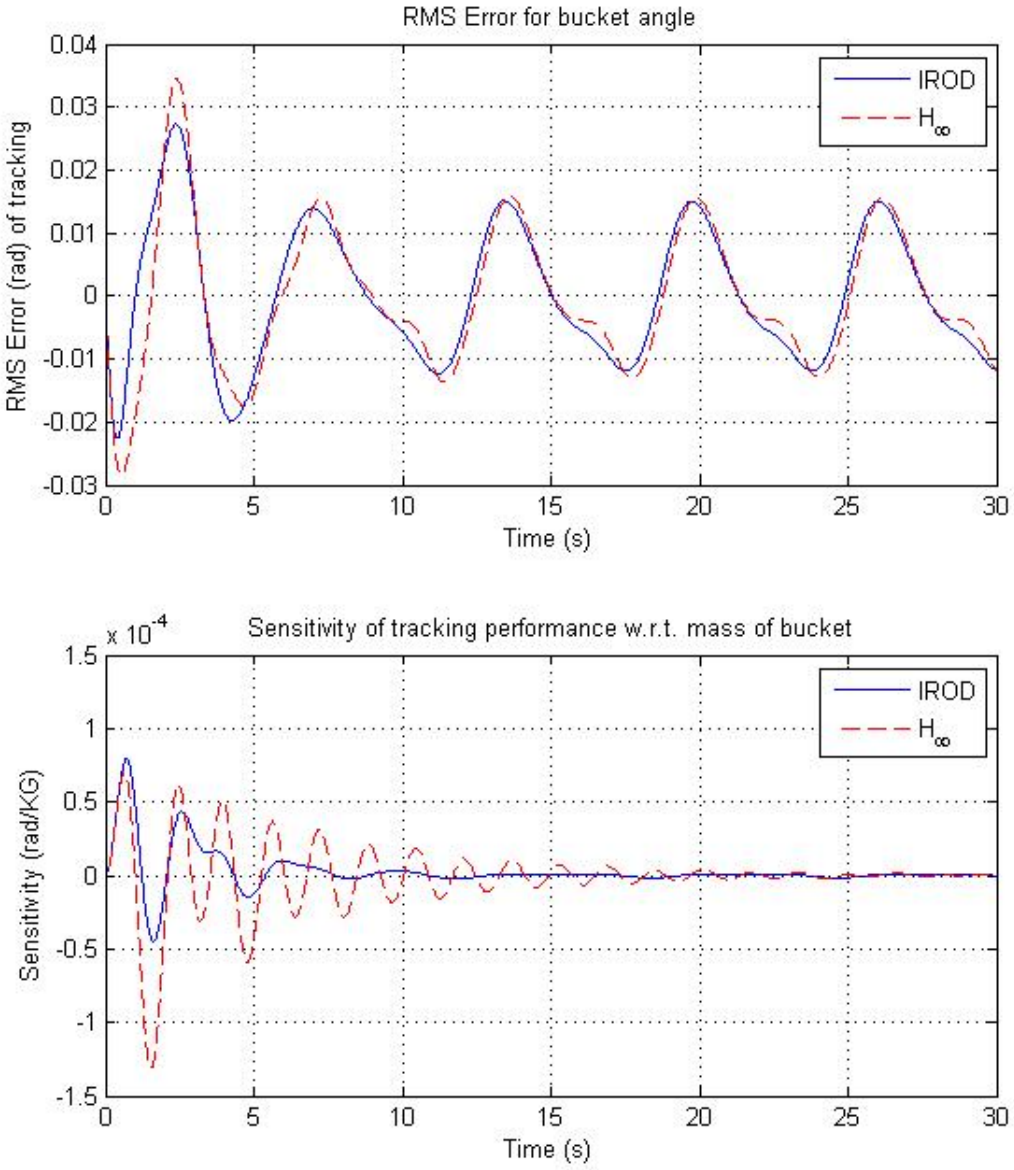

Figure 4.8 Comparison between the performance and sensitivity of sequential $\mathcal{H}_\infty$design and IROD of excavator.

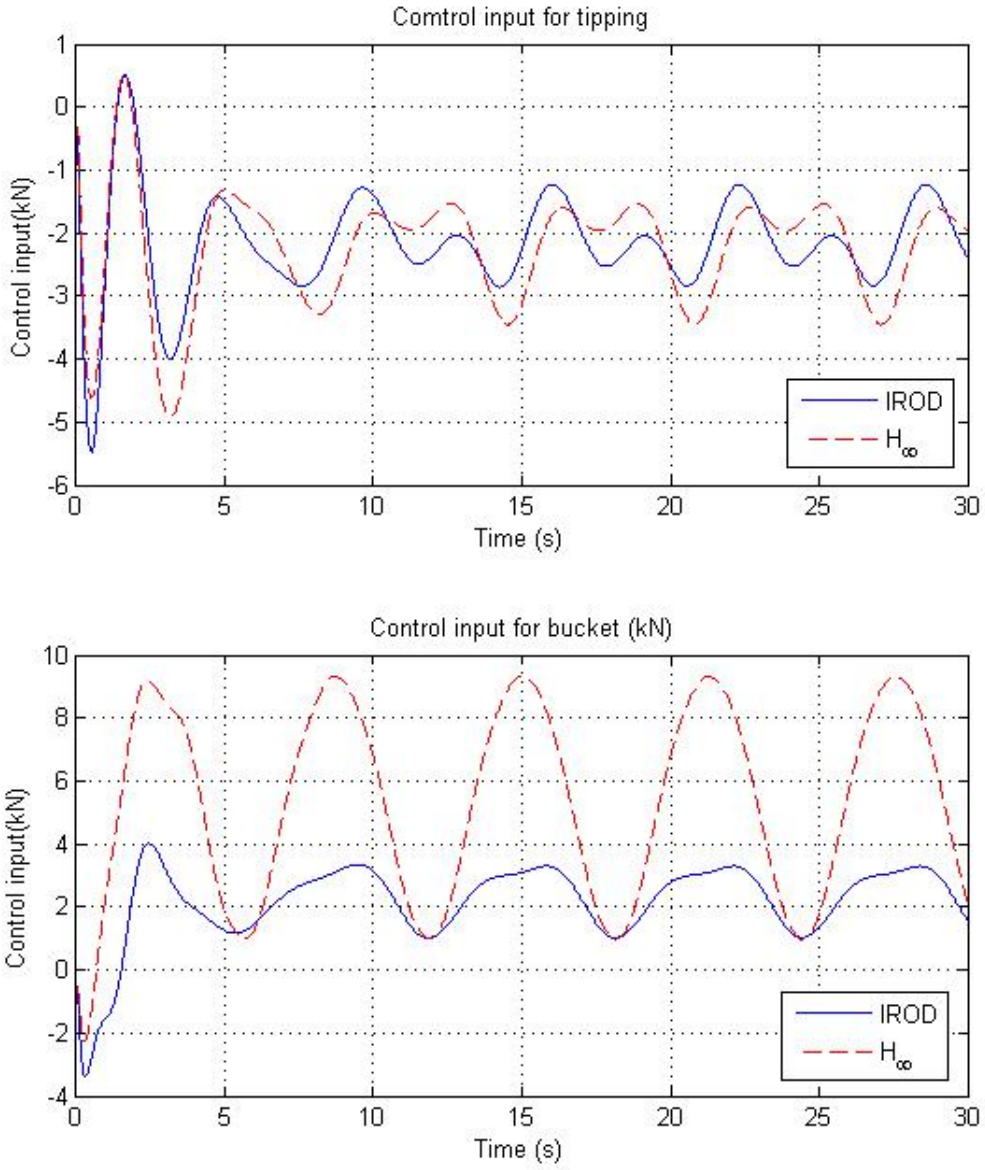

Figure 4.9 Comparison between control input in sequential $\mathcal{H}_\infty$design and IROD of excavator

CHAPTER 5. ROBUST FEEDBACK LINEARIZATION

For nonlinear systems with parametric uncertainties and which cannot be linearized at an operating point, a sensitivity based robust feedback linearization method is proposed in this chapter. The systems considered here are assumed to be feedback linearizable and minimum phase.

The nonlinear systems considered here are of the form -

$$\begin{aligned} \dot{x} &= f(x,b) + g(x,b)u \\ y &= h(x,b) \end{aligned} \tag{5.1}$$

where, $x \in \Re^n$ is state vector, $b \in \Re$ is a parameter, $f : \Re^{n+1} \to \Re^n$, $g : \Re^{n+1} \to \Re$ and $h : \Re^{n+1} \to \Re$ are continuously differentiable functions. The parameter b in system Eq. (5.1) is uncertain or subject to change due to wear and tear. The robust feedback linearization is explained for a single uncertain parameter but, it can be extended to vector of parameters. The sensitivity of a nonlinear system is defined as a change in the output as a function of small change in the parameter, hence the sensitivity dynamics is given by-

$$\begin{aligned} \dot{x_b} &= f_b(x, x_b, b) + g_b(x, x_b, b)u \\ y_b &= h_b(x, x_b, b) \end{aligned} \tag{5.2}$$

where $x_b \in \Re^n$ is a sensitivity state vector, subscript b indicates full derivative with respect to b, that is $(.)_b = \frac{\partial(.)}{\partial b} + \frac{\partial(.)}{\partial x} x_b$, and y_b is the sensitivity of output.

5.1 Feedback Linearization of Augmented Sensitivity Dynamics

First, we consider only the linear dynamics and assume that the nonlinear system is minimum phase. The feedback linearized dynamics of the nominal nonlinear system consists of n integrators and one input. For the nominal system performance, sufficiently high gain controller used in negative feedback can stabilize the closed loop system and can be used for tracking. Any other controller can also be designed for better tracking, but in this research we assumed only gain K used in negative feedback. The closed loop system dynamics is then -

$$\dot{\zeta} = A\zeta + BK(w - \zeta_1) \tag{5.3}$$

since $\nu = K(w - y) = K(w - \zeta_1)$, where w is the exogenous reference input. Also, for nominal system $\nu = L_f^r h + L_g^r h u_0$, therefore

$$u = \frac{K(w - h) - L_f^r h}{L_g^r h} \tag{5.4}$$

5.1.1 Robust Control

With the same gain, u_b can be computed from Eq. (5.38), in terms of u and ν_b. The same K also stabilizes the sensitivity dynamics since linear sensitivity dynamics is also a set of n integrators with input ν_b. In case of sensitivity dynamics the desired signal is 0, since the reference signal is independent of parameter, i.e. $w_b = 0$. As discussed in the previous section, the control input u_b is the direction towards minimum sensitivity. The step size K_2 can be chosen such that the closed loop system remains stable and the sensitivity dynamics converges fast enough. Fig. (5.1) shows the control signal flow diagram. In this method, the controller includes sensitivity dynamics which is given by Eq. (5.5).

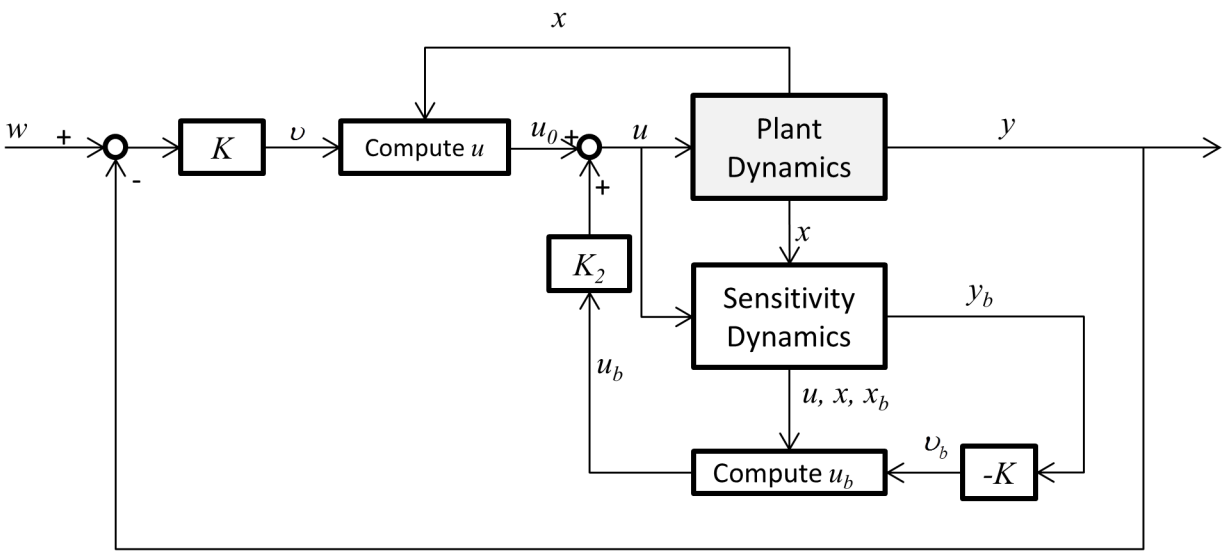

Figure 5.1 Robust feedback linearization control structure

5.2 Robust Control Design

5.2.1 Robust Control Problem Structure

In the sensitivity based robust optimal control synthesis problem, the sensitivity with respect to the uncertain parameter is minimized. Sensitivity dynamics is either used in the process of optimal control synthesis, or it can be used within the controller. In the case of feedback controller, the control input u is considered parameter dependent because the parameter dependent output is used for control input calculation. The sensitivity augmented system with parameter dependent control input is given by -

$$\begin{aligned} \dot{x} &= f(x,b) + g(x,b)u(x) \\ \dot{x}_b &= f_b(x,x_b,b) + g_b(x,x_b,b)u(x) + g(x,b)u_b(x) \\ y &= h(x,b) \\ y_b &= h_b(x,x_b,b) \end{aligned} \tag{5.5}$$

where, $u_b = \frac{du}{db}$ is the variation in control input. Let the augmented state vector be- $\mathcal{X} = [x^T, x_b^T]^T$. The system in Eq. (5.5) has two inputs u and u_b, and two outputs y and y_b. The objective of robust feedback control is to design a controller which minimizes the sensitivity and improve performance. The robustness is added through adapting the control input, which is assumed parameter independent, to minimize the sensitivity. The objective function for robustness is set to be -

$$J(u) = \frac{1}{2}\frac{(u(b_0) - u(b))^2}{b_0 - b} \tag{5.6}$$

Control input u is depends affinely on output y since a feedback control is designed, hence minimum of error in u, also gives minimum in error in y. If we take limit as $b_0 - b \to 0$, then the direction towards minimum of the objective function is -

$$\lim_{(b_0 - b)\to 0} \nabla_u J(u) = -u_b \tag{5.7}$$

A suitable step size K_2 can be used, such that the closed loop system remains stable. The stability and feedback linearization for sensitivity augmented system is explained in next three subsections.

5.2.2 Notation

A Lie derivative of function $h(x, b)$ along $f(x, b)$ with respect to x is defined as - $L_f h = \frac{\partial h}{\partial x}^T f(x, b)$ The full derivative of Lie derivative with respect to parameter b is given by -

$$\frac{dL_f h(x, b)}{db} = \frac{\partial L_f h(x, b)}{\partial b} + \frac{\partial L_f h(x, b)}{\partial x} x_b \tag{5.8}$$

since both function f and h are continuously differentiable, the order of derivatives can be exchanged, and hence from product rule

$$\frac{dL_f h(x,b)}{db} = L_{f_b} h(x,b) + L_f h_b(x,b) \tag{5.9}$$

also,

$$\frac{dL_g L_f h(x)}{db} = L_{g_b} L_f h(k) + L_g L_{f_b} h(x) + L_g L_f h_b(x) \tag{5.10}$$

and

$$\frac{dL_f^k h(x)}{db} = \frac{\partial}{\partial x}\frac{d}{db} L_f^{k-1} h(x) f(x) \tag{5.11}$$

where, the subscript b indicates full derivative, i.e.

$$L_{f_b} h(x,b) = \left[\frac{\partial h(x,b)}{\partial x}\right]^T \frac{\partial f(x,b)}{\partial b} + \left[\frac{\partial h(x,b)}{\partial x}\right]^T \left[\frac{\partial f(x,b)}{\partial x}\right]^T x_b \tag{5.12}$$

$$L_f h_b(x,b) = \left[\frac{\partial^2 h(x,b)}{\partial b \partial x}\right]^T f(x,b) + \left[\frac{\partial^2 h(x,b)}{\partial^2 x} x_b\right]^T f(x,b) \tag{5.13}$$

Dependence of f, h and g on x and b is not explicitly written hereon, but it is assumed. Another important identity that follows is -

$$\begin{aligned} \frac{\partial f_b}{\partial x_b} &= \frac{\partial}{\partial x_b}\left(\frac{\partial f}{\partial b} + \frac{\partial f}{\partial x} x_b\right) \\ \frac{\partial f_b}{\partial x_b} &= \frac{\partial f}{\partial x} \end{aligned} \tag{5.14}$$

Similar is true for Lie derivatives -

$$\frac{\partial}{\partial x_b}\frac{d}{db} L_f h = \frac{\partial}{\partial x} L_f h \tag{5.15}$$

5.2.3 Feedback Linearization

Theorem 1. *If the nonlinear system in Eq. (5.1) has relative degree r then the relative degree of sensitivity augmented system in Eq. (5.5) is $[r, r]$.*

Proof. From the definition of relative degree - $L_g L_f^{k-1} h(x)u = 0,\ \forall\ 0 \leq k < r$ and $\forall x$ in a neighborhood D of operating point x_0, b_0 and u_{0_0} and $L_g L_f^l h(x)u \neq 0\ \forall\ r-1 \leq l \leq n$ in the neighborhood D.

$$\Rightarrow \frac{dL_g L_f^{k-1} h(x)u}{db} = 0\ \forall 0 \leq k < r \tag{5.16}$$

also,

$$\frac{dL_g L_f^l h(x)u}{db} = L_{g_b} L_f^l hu + L_g \frac{dL_f^l h}{db} u + L_g L_f^k h u_b \tag{5.17}$$

In order for above quantity to be zero $\forall u$ and u_b, multipliers of u and u_b should be independently zero, but $L_g L_f^l h \neq 0$, hence

$$\Rightarrow \frac{dL_g L_f^l h(x)u}{db} \neq 0\ \forall\ r-1 \leq l \leq n \tag{5.18}$$

Now, compute the relative degree for system in Eq. (5.5). The 1^{st} time derivative of y_b is given by-

$$\dot{y}_b = \frac{\partial h_b}{\partial x}\dot{x} + \frac{\partial h_b}{\partial x_b}\dot{x}_b \tag{5.19}$$

Substituting for $\dot{x}$ and $\dot{x}_b$ from Eq. (5.5) and from identity Eq. (5.14)

$$\begin{aligned} \dot{y}_b &= \frac{\partial h_b}{\partial x}(f + gu_0 + gu_b) + \frac{\partial h}{\partial x}(f_b + g_b u_0 + g u_b) \\ &= \frac{d}{db}(L_f h + L_g h u) \end{aligned} \tag{5.20}$$

If $\frac{dL_g hu}{db}$ is zero, the second derivative of y_b is given by -

$$\begin{aligned} y_b^{(2)} &= \frac{\partial}{\partial x}\left(\frac{dL_f h}{db}\right)\dot{x} + \frac{\partial}{\partial x_b}\left(\frac{dL_f h}{db}\right)\dot{x}_b \\ &= \frac{\partial}{\partial x}\left(\frac{dL_f h}{db}\right)(f + gu_0 + gu_b) + \frac{\partial}{\partial x_b}\left(\frac{dL_f h}{db}\right)(f_b + g_b u_0 + g u_b) \\ &= \frac{d}{db}(L_f^2 h + L_g L_f h u) \end{aligned} \tag{5.21}$$

Similarly, the k^{th} derivative of $\dot{y}_b$, if $L_g L_f^{k-2} hu$ is zero, is given by -

$$y_b^{(k)} = \frac{d}{db}(L_f^k h + L_g L_f^{k-1} hu) \tag{5.22}$$

Hence,the $y_b^{(k)}$ is independent of u iff $\frac{dL_g L_f^{k-1} hu}{db} = 0$, i.e. the relative degree of sensitivity dynamics is s if $\frac{dL_g L_f^{k-1} hu}{db} = 0 \; \forall \; 0 \leq k < s$ and $\frac{dL_g L_f^{l} hu}{db} \neq 0 \; \forall \; s \leq l \leq n$. From Eq. (5.16) and Eq. (5.18), $s = r$. Which proves the theorem. □

Theorem 2. *Consider the system in Eq. (5.5) and it has relative degree $[r, r]$, where $r < n$ in $D \in \Re^{2n}$, then $\forall \; \mathcal{X} \in D$, there exists a neighborhood $\mathcal{N} = N \oplus N_b$ of $\mathcal{X}_0$ and smooth functions $\phi_1(x, b), \phi_2(x, b), \phi_3(x, b), \ldots, \phi_{n-r}(x, b)$ such that*

$$L_g \phi_i(x, b) = 0, \; \forall \; 1 \leq i \leq n \; \exists [x, x_b] \in \mathcal{N}$$

and the mapping

$$T = \begin{bmatrix} T_N \\ T_b \end{bmatrix} \tag{5.23}$$

restricted to $\mathcal{N}$ is a deffeomorphism on $\mathcal{N}$ where,

$$T_N(x, x_b, b) = \left[\begin{array}{c} \phi_1(x, b) \\ \phi_2(x, b) \\ \vdots \\ \phi_{n-r}(x, b) \\ \hdashline h \\ \vdots \\ L_f^{r-1} h \end{array}\right] = \begin{bmatrix} \eta \\ \zeta \end{bmatrix} \tag{5.24}$$

and

$$T_b(x, x_b, b) = \begin{bmatrix} \phi_{1_b}(x, b) \\ \phi_{2_b}(x, b) \\ \vdots \\ \phi_{(n-r)_b}(x, b) \\ \hdashline h_b \\ \vdots \\ \frac{dL_f^{r-1}h}{db} \end{bmatrix} = \begin{bmatrix} \eta_b \\ \zeta_b \end{bmatrix} \tag{5.25}$$

Proof. In order to prove that T is a diffeomorphism, we need to prove that T^{-1} is non-singular in $\mathcal{N}$. We know that for a neighbourhood N of x_0, the transformation T_N is a diffeomorphism. The Jacobian of T is given by -

$$\nabla_{\mathcal{X}} T = \begin{bmatrix} \frac{\partial T_N}{\partial x} & 0 \\ \frac{\partial T_b}{\partial x} & \frac{\partial T_b}{\partial x_b} \end{bmatrix} \tag{5.26}$$

It can be proved from identity in Eq. (5.14) that $\frac{\partial T_b}{\partial x_b} = \frac{\partial T_N}{\partial x}$.

$$\nabla_{\mathcal{X}} T = \begin{bmatrix} \frac{\partial T_N}{\partial x} & 0 \\ \frac{\partial T_b}{\partial x} & \frac{\partial T_N}{\partial x} \end{bmatrix} \tag{5.27}$$

It can be seen in Eq. (5.27) that the matrix is lower block triangular with identical diagonal blocks. This proves that $\nabla_{\mathcal{X}} T$ is invertible in a neighborhood $N \oplus N_b$.

□

5.2.4 Zero Dynamics

The state vector $\mathcal{X}$ is transformed into new states $[\eta^T,\ \zeta^T,\ \eta_b^T,\ \zeta_b^T]^T = \Xi$ by $\Xi = T(\mathcal{X}, b)$. The dynamics of η is -

$$\begin{aligned}\dot{\eta} &= \frac{\partial \phi}{\partial x}(f+gu) \\ \dot{\eta} &= f_0(\eta,\zeta) \end{aligned} \tag{5.28}$$

since $L_g\phi u = 0$ in neighborhood N.

This also imply that -

$$\frac{dL_g\phi u}{db} = 0 \tag{5.29}$$

in a neighborhood $\mathcal{N}$.

The dynamics for η_b is given by -

$$\begin{aligned}\dot{\eta}_b &= \frac{\partial \phi_b}{\partial x}(f+gu) + \frac{\partial \phi_b}{\partial x_b}(f_b + g_b u_0 + g u_b) \\ &= \frac{\partial \phi_b}{\partial x} f + \frac{\partial \phi}{\partial x} f_b + \frac{\partial \phi}{\partial x} g_b u + \frac{\partial \phi}{\partial x} g u_b \end{aligned}$$

Now from identity Eq. (5.14),

$$\begin{aligned}\dot{\eta}_b &= \frac{d}{db}\left[\frac{\partial \phi}{\partial x} f\right] + \frac{d}{db}\left[\frac{\partial \phi}{\partial x} g u\right] \\ &= \frac{d}{db}\left[\frac{\partial \phi}{\partial x} f\right] \\ \dot{\eta}_b &= f_{0_b}(\eta,\zeta,\eta_b,\zeta_b) \end{aligned} \tag{5.30}$$

Theorem 3. *If the zero dynamics given by $f_0(\eta,0)$ is asymptotically stable in a neighborhood D_η of operating point η_0 then the sensitivity zero dynamics $f_{0_b}(\eta,0,\eta_b,0)$ is also asymptotically stable at in a neighborhood of operating point $[\eta^T,\ \eta_b^T]^T = [\eta_0^T, \eta_{b0}^T]^T$ where*

$$\eta_{b_0} = \frac{\partial f_0(\eta_0,0)}{\partial b}\left[\left.\frac{\partial f_0(\eta,0)}{\partial \eta}\right|_{\eta=\eta_0}\right]^{-1} \tag{5.31}$$

. In other words if system in Eq. (5.1) is minimum phase in domain D_η then the sensitivity augmented system in Eq. (5.5) is also minimum phase in domain $D_\eta \oplus D_{\eta_b}$.

Proof. From [56], a neighborhood of operating point is asymptotically stable if

$$eig\left(\left.\frac{\partial f_0(\eta,0)}{\partial \eta}\right|_{\eta=\eta_0}\right) < 0 \tag{5.32}$$

The zero dynamics of sensitivity augmented system is given by simultaneously solving Eq. (5.28) and Eq. (5.30) simultaneously, hence the Jacobian of zero dynamics of augmented system is -

$$\nabla_{[\eta^T,\, \eta_b^T]^T}\begin{bmatrix} f_0(\eta,0) \\ f_{0_b}(\eta,0,\eta_b,0)\end{bmatrix} = \left.\begin{bmatrix} \frac{\partial f_0(\eta,0)}{\partial \eta} & 0 \\ \frac{\partial f_{0_b}(\eta,0,\eta_b,0)}{\partial \eta} & \frac{\partial f_{0_b}(\eta,0,\eta_b,0)}{\partial \eta_b}\end{bmatrix}\right|_{\eta=\eta_0,\, \eta_b=\eta_{b_0}} \tag{5.33}$$

From Eq. (5.30),

$$f_{0_b}(\eta,0,\eta_b,0) = \frac{d}{db} f_0(\eta,0)$$

Hence, from identity Eq. (5.14) -

$$\nabla_{[\eta^T,\, \eta_b^T]^T}\begin{bmatrix} f_0(\eta,0) \\ f_{0_b}(\eta,0,\eta_b,0)\end{bmatrix} = \left.\begin{bmatrix} \frac{\partial f_0(\eta,0)}{\partial \eta} & 0 \\ \frac{\partial f_{0_b}(\eta,0,\eta_b,0)}{\partial \eta} & \frac{\partial f_0(\eta,0)}{\partial \eta}\end{bmatrix}\right|_{\eta=\eta_0,\, \eta_b=\eta_{b_0}} \tag{5.34}$$

The Jacobian in Eq. (5.34) has lower block triangular structure and the blocks on diagonal are identical. Which means the Jacobian has repeated eigen values, and those are equal to the eigen values of $\left.\frac{\partial f_0(\eta,0)}{\partial \eta}\right|_{\eta=\eta_0}$. Hence from Eq. (5.32) -

$$eig\left(\nabla_{[\eta^T,\, \eta_b^T]^T}\begin{bmatrix} f_0(\eta,0) \\ f_{0_b}(\eta,0,\eta_b,0)\end{bmatrix}\right) < 0 \tag{5.35}$$

which proves the theorem □

5.2.5 Linear System

The linear dynamics in ζ and ζ_b with minimum phase nonlinear nonlinear dynamics in η and η_b is -

$$\begin{aligned}
\dot{\eta} &= f_0(\eta, \zeta) \\
\dot{\eta}_b &= F_{0_b}(\eta, \zeta, \eta_b, \zeta_b) \\
\dot{\zeta} &= A\zeta + B\nu \\
\dot{\zeta}_b &= A\zeta_b + B\nu_b \\
y &= \zeta_1 \\
y_b &= \zeta_{b_1}
\end{aligned} \tag{5.36}$$

where, A is a $n \times n$ matrix with off diagonal ones, which is a normal form of n integrators, $B_{1\times n} = [0,\ 0,\ \ldots,\ 1]^T$ and

$$\nu = L_f^r h + L_g L_f^{r-1} h u \tag{5.37}$$

and

$$\nu_b = \frac{d}{db} L_f^r h + \frac{d}{db}(L_g L_f^{r-1} h u) \tag{5.38}$$

5.3 Application to Hydraulic Actuator

The sensitivity based robust feedback linearization method is implemented for hydraulic nonlinear system with linear spring mass damper plant model. The hydraulic actuator consists of piston, cylinder and 4-way spool valve. The schematic diagram of the hydraulic system is shown in Fig. (5.2). The explanation and values of variables are given in table 5.1. The values of states, input, output and flow are the initial operating conditions. The fluid density ρ is assumed to be uncertain. Hence the objective is to

Table 5.1 Explanation of variables

Variable	Description	Value
m_a	Mass	10 Kg
m_e	Mass	5 Kg
k_e	Spring constant	100 N/m
k_s	Spring constant	100 N/m
d_o	Damping constant	1000 Ns/m
d_s	Damping constant	10 Ns/m
d_e	Damping constant	100 Ns/m
P_s	Pump pressure	2×10^7pa
P_e	Tank pressure	0
Q_A	Flow through chamber orifice	0
Q_B	Flow through piston side orifice	0
ρ	Fluid density	961.87 Kg/m^3
β	Bulk modulus	1.2485×10^9 Pa
VO_A	Cylinder chamber dead volume	1×10^{-4} m^{-3}
VO_B	Piston chamber dead volume	1×10^{-4} m^{-3}
w	Valve maximum width	0.005 m
C_d	Discharge coefficient	0.62
A_A	Cylinder cross section area	0.125 m^2
A_B	Piston area	0.125 m^2
l_{max}	Piston stroke	$3m$
x_{sp}	Spool valve position (control input)	0 m
P_A	Chamber pressure (state)	$P_s/2$
P_B	Piston side pressure (state)	$P_s/2$
x_p	piston position (state)	1.5 m
f_a	Hydraulic force (output)	0 N

track the desired x_e and minimize the sensitivity of tracking with respect to variations in fluid density. The nominal system dynamics is taken from [74]

The spring mass damper part of dynamics is given by -

$$\begin{aligned} m_a\ddot{x}_p &= f_a - d_s(\dot{x}_p - \dot{x}_e) - d_0\dot{x}_p - k_s(x_p - x_e) \\ m_e\ddot{x}_e &= d_s(\dot{x}_p - \dot{x}_e) - d_e\dot{x}_e + k_s(x_p - x_e) - k_e x_e \end{aligned} \tag{5.39}$$

where f_a is the force applied by the hydraulic actuator. The hydraulic dynamic equations are -

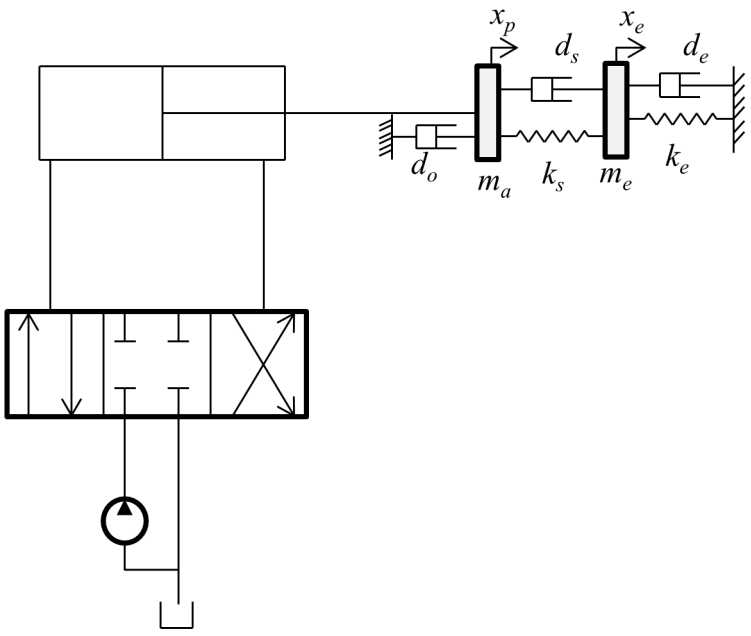

Figure 5.2 Hydraulic system dynamics schematic diagram

$$f_a = P_A A_A - P_B A_B \tag{5.40}$$

$$\dot{P}_A = \frac{\beta}{V0_A + A_A x_p}(Q_A - A_A \dot{x}_p) \tag{5.41}$$

$$\dot{P}_B = \frac{\beta}{V0_B + A_B(l_{max} - x_p)}(-Q_B + A_B \dot{x}_p) \tag{5.42}$$

and the flow equations are -

$$Q_A = C_d w x_{sp} \sqrt{\frac{2}{\rho}}(\sqrt{P_s - P_A} sg(x_{sp}) + \sqrt{P_A - P_e} sg(-x_{sp})) \tag{5.43}$$

$$Q_B = C_d w x_{sp} \sqrt{\frac{2}{\rho}}(\sqrt{P_B - P_e} sg(x_{sp}) + \sqrt{P_s - P_B} sg(-x_{sp})) \tag{5.44}$$

where

$$sg(x_{sp}) = \begin{cases} 1 & \text{if } x_{sp} > 0 \\ 0 & \text{if } x_{sp} \leq 0 \end{cases} \tag{5.45}$$

The controller for the full system is designed in two steps; in the first step, tracking controller is designed for linear mechanical system assuming force as the input and then force tracking controller is designed for hydraulic actuator using sensitivity based robust feedback linearization. Figure 5.3 shows the structure of the nominal feedback linearized controller, where K_{track} is the tracking controller and K_{inner} is the force controller.

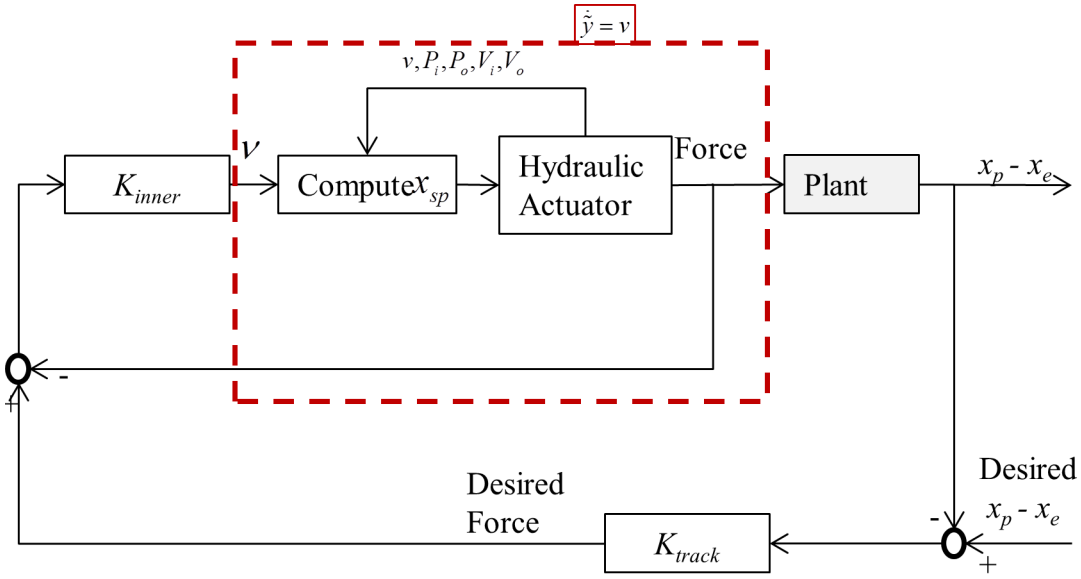

Figure 5.3 Control structure of feedback linearization for hydraulic actuator

5.3.1 Feedback Control Design

Since the plant model is simply a linear spring damper, a PID controller is designed for K_{track} and force controller is $K_{inner} = 10^7$

$$K_{track} = 10^4 \frac{1 + 3.7s}{s} \tag{5.46}$$

The feedback linearization is of Eq. (5.40) is achieved by transforming states P_A and P_B to new states, $\tilde{P}_A$ and $\tilde{P}_B$. This transformation cancels the velocity terms, $\dot{x}_p$ in Eq. (5.41) and Eq. (5.42). The state transformation used here is -

$$\begin{aligned} \tilde{P}_A &= P_A + \beta ln(A_A x_p + V0_A) \\ \tilde{P}_B &= P + B + \beta ln(A_B(l_{max} - x_p) + V0_B) \end{aligned} \tag{5.47}$$

Hence, the force is transformed into -

$$\tilde{y}_f = f_a + A_A \beta ln(A_A x_p + V0_A) - A_B \beta ln(A_B(l_{max} - x_p) + V0_B) \tag{5.48}$$

The feedback linearized system then reduces to

$$\dot{\tilde{y}} = \nu \tag{5.49}$$

From Eq. (5.47) and Eq. (5.48), expression for ν is obtained in therms of states and actual control input x_{sp}.

$$\nu = \begin{cases} x_{sp}\sqrt{\frac{2}{\rho}}\beta C_d w \left(\frac{A_A}{A_A x_p + V0_A}\sqrt{P_s - P_A} + \frac{A_B}{A_B(l_{max}-x_p)+V0_B}\sqrt{P_B - P_e} \right) & x_{sp} > 0 \\ 0 & x_{sp} = 0 \\ x_{sp}\sqrt{\frac{2}{\rho}}\beta C_d w \left(\frac{A_A}{A_A x_p + V0_A}\sqrt{P_A - P_e} + \frac{A_B}{A_B(l_{max}-x_p)+V0_B}\sqrt{P_s - P_B} \right) & x_{sp} < 0 \end{cases} \tag{5.50}$$

The actual control input x_{sp} can be computed from ν because both have the same sign. The K_{inner} is designed to reduce the error between desired $\tilde{y}$ and actual $\tilde{y}$. That is input to K_{inner} is $\tilde{y}_{desired} - \tilde{y}_{actual}$ which is $e_f = f_{desired} - f_a$. The control input ν is therefore -

$$\nu = K_{inner}(\tilde{y}_{desired} - \tilde{y}_{actual}) = K_{inner} e_f \tag{5.51}$$

5.3.2 Robust Feedback Lineariztion

In order to change the control input to uncertainties in fluid density we need to find the sensitivity of x_{sp} to changes in ρ. As explained in the previous section, first we find sensitivity dynamics with respect to ρ. From hereon subsrcript ρ represents full derivative with respect to ρ.

The sensitivity of force f_a is given by differentiating the output equation Eq. (5.40).

$$f_{a_\rho} = P_{A_\rho} A_A - P_{B_\rho} A_B \tag{5.52}$$

Note here, that desired F_ρ is zero. The sensitivity dynamics is obtained by differentiating Eq. (5.41) and Eq. (5.42).

$$\begin{aligned} \dot{P}_{A_\rho} &= \frac{-\beta}{(V0_A + A_A x_p)^2} A_A x_{p_\rho} (Q_A - A_A \dot{x}_p) \\ &\quad + \frac{\beta}{(V0_A + A_A x_p)} (Q_{A_\rho} - A_A \dot{x}_{p_\rho}) \end{aligned} \tag{5.53}$$

$$\begin{aligned} \dot{P}_{B_\rho} &= \frac{\beta}{(V0_B + A_B(l_{max} - x_p))^2} A_B x_{p_\rho} (-Q_B + A_B \dot{x}) \\ &\quad \frac{\beta}{V0_B + A_B(l_{max} - x_p)} (-Q_{B_\rho} + A_B \dot{x}_{p_\rho}) \end{aligned} \tag{5.54}$$

The flow sensitivities are calculated separately at $x_{sp} < 0$ and $x_{sp} > 0$. At $x_{sp} = 0$ the flow is zero hence, the flow sensitivity is zero. The discontinuity at $x_{sp} = 0$ is included in the equations as three different continuous cases, instead of differentiating the $sg(x_{sp})$ functional.

$$
\begin{aligned}
Q_{A_\rho} &= C_d w x_{sp_\rho} \sqrt{\frac{2}{\rho}} (\sqrt{P_s - P_A} sg(x_{sp}) + \sqrt{P_A - P_e} sg(-x_{sp})) \\
&\quad - C_d w x_{sp} \sqrt{\frac{1}{2\rho^3}} (\sqrt{P_s - P_A} sg(x_{sp}) + \sqrt{P_A - P_e} sg(-x_{sp})) \\
&\quad + C_d w x_{sp} \sqrt{\frac{1}{2\rho}} (\frac{-1}{(P_s - P_A)^{1/2}} P_{A_\rho} sg(x_{sp}) + \frac{1}{(P_A - P_e)^{1/2}} P_{A_\rho} sg(-x_{sp})) \quad (5.55) \\
Q_{B_\rho} &= C_d w x_{sp_\rho} \sqrt{\frac{2}{\rho}} (\sqrt{P_B - P_e} sg(x_{sp}) + \sqrt{P_s - P_B} sg(-x_{sp})) \\
&\quad - C_d w x_{sp} \sqrt{\frac{1}{2\rho^3}} (\sqrt{P_B - P_e} sg(x_{sp}) + \sqrt{P_s - P_B} sg(-x_{sp})) \\
&\quad + C_d w x_{sp} \sqrt{\frac{1}{2\rho}} (\frac{1}{(P_B - P_e)^{1/2}} P_{B_\rho} sg(x_{sp}) + \frac{-1}{(P_s - P_B)^{1/2}} P_{B_\rho} sg(-x_{sp})) \quad (5.56)
\end{aligned}
$$

The sensitivity of x_p and x_e can be obtained by differentiating Eq. (5.39). Remember that f_a and pressures are functions of ρ. The nonlinear dynamical equations Eq. (5.53) and Eq. (5.54) along with output equation Eq. (5.52) can be output-state feedback linearized by the transformation obtained by differentiating the transformation in Eq. (5.48), that is

$$
\tilde{y}_{f_\rho} = f_{a_\rho} + A_A \frac{\beta}{A_A x_p + V0_A} A_A x_{p_\rho} + A_B \frac{\beta}{A_B (l_{maz} - x_p) + V0_B} A_B x_{p_\rho} \quad (5.57)
$$

This transformation leads to linear system -

$$
\dot{\tilde{y}}_\rho = \nu_\rho \quad (5.58)
$$

where, ν_ρ can be obtained from the transformation Eq. (5.57) in terms of x_{sp} and x_{sp_ρ}. From this relationship, x_{sp_ρ} can be obtained as function of states, sensitivity states and ν_ρ. The simpler way of obtaining ν_ρ is by separately taking full derivative of Eq. (5.50) with respect to ρ for all three cases. From the nominal closed loop system, i.e. Eq. (5.51), and since desired $\tilde{y}_\rho$ is zero -

$$
\nu_\rho = K_{inner} \tilde{y}_\rho \quad (5.59)
$$

The control input correction x_{sp_ρ} is then used as a correction step in actual control input x_{sp}.

5.4 Results

A controller was designed for the system shown in Fig. (5.2) for tracking x_e and minimizing sensitivity with respect to variations in fluid density. The desired x_e is a sinusoidal input and variation in ρ was assumed to be 0.1% from nominal value. The step size, K_2, for faster convergence was chosen to be 10^3.

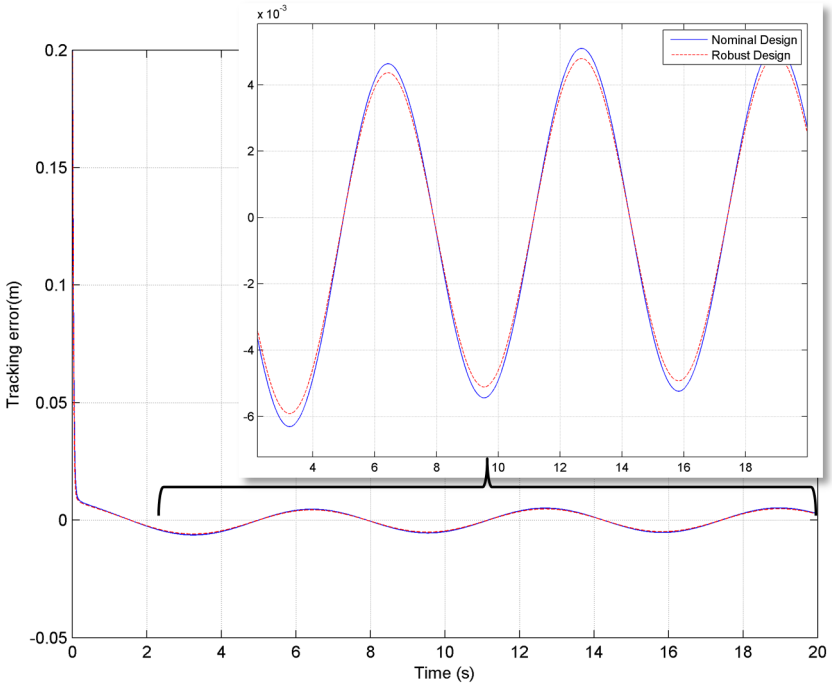

Figure 5.4 Tracking error between desired and actual x_e

Fig. (5.4) shows the tracking errors for nominal design and robust design. The input was sinusoidal with frequency $1rad/sec$, amplitude of $0.1m$ and bias of $0.2m$.

The sensitivity of tracking and force are compared between nominal design and robust design in Fig. (5.5) and Fig. (5.6), respectively. The figures show that the sensitivity to variations in fluid density is reduced by adding robustness correction using sensitivity

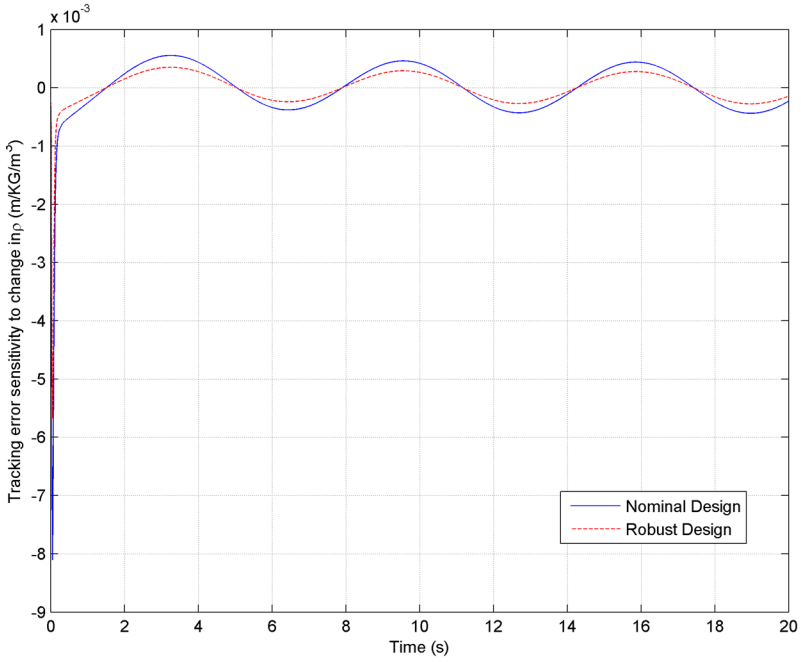

Figure 5.5 Comparison between sensitivity of nominal and robust designs

Table 5.2 Comparison between robust and nominal feedback linearization

	Nominal Design	Robust Design	% Improvement
RMS Tracking Error	2.9330×10^{-7}	1.2619×10^{-7}	56.97
RMS Tracking Sensitivity	6.0487×10^{-5}	5.6739×10^{-5}	6.19
RMS Force Sensitivity	168.93	85.460	49.41
10% Tolerance Band	$\pm 4.8490 \times 10^{-4}$	$\pm 5.1693 \times 10^{-4}$	6.6057

dynamics. The RMS tracking error, RMS sensitivity, and RMS sensitivity of force are given in table 5.2. The tolerance band for nominal design is calculated by allowing tracking error to increase by 10%, and the tolerance band for robust design is calculated by letting tracking error go up by the same margin.

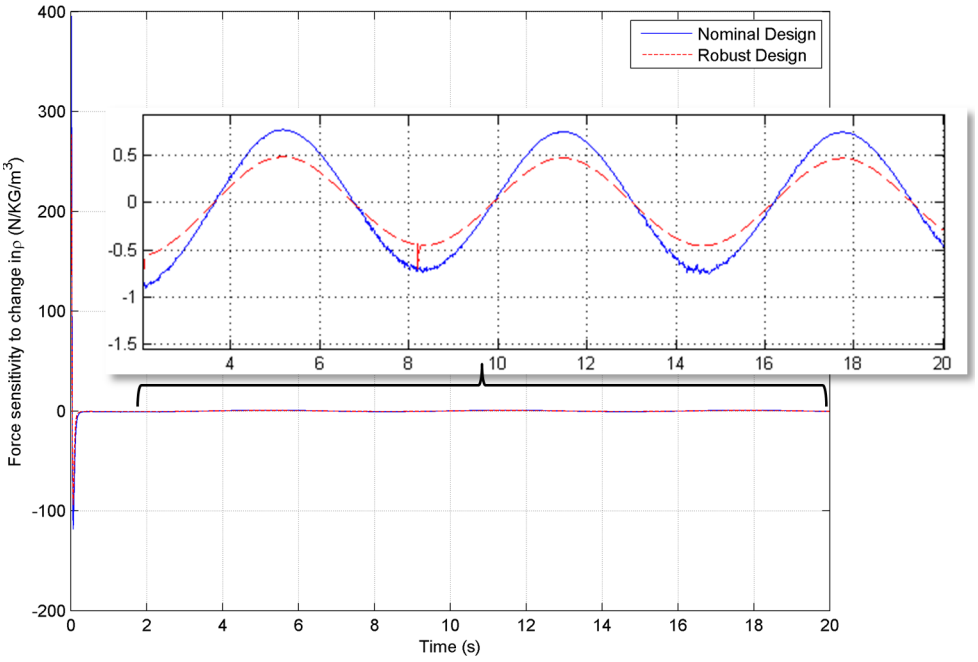

Figure 5.6 Comparison between nominal and robust designs in terms of sensitivity of force

CHAPTER 6. CONCLUSIONS AND FUTURE WORK

In this research, a novel methodology is proposed for Integrated Robust Optimal Design (IROD) of linear systems using a combination of traditional sensitivity theory and relatively modern developments in Linear Matrix Inequalities (LMI) and convex optimization methods. This methodology is a viable alternative to existing sequential robust control design techniques. Although this method requires linearization of nonlinear systems at each step in the outer optimization loop, an efficient approach is proposed to facilitate linearization of DAE using symbolic computation. As this method provides techniques to model the system with uncertain parameters in a symbolic form, it eliminates the need of repetitive linearizations. The use of sensitivity theory for IROD eliminates the need to estimate uncertainty bounds for all possible system configurations. The uncertainty estimates are generally overly conservative, but sensitivity minimal design is the least conservative approach for robust synthesis. Since the algorithm used to solve BMI constrained problem guarantees local convergence, the integrated design is also guaranteed to be locally optimal. The global solution strategies like genetic algorithm and particle swarm method do not guarantee convergence in polynomial time since the problem is non-convex and np-hard. The proposed methodology can also provide Pareto optimal controllers for performance, robustness and control power. The uncertainties other than parametric uncertainties can also be used in this formulation using some approximations; for example, uncertainty in the performance due to unknown delays can be modeled by Pade's approximation.

The efficiency of IROD methodology is demonstrated by applications to combine

harvester header height control problem and excavator bucket level control problem. The proposed method is compared with the nominal and robust $\mathcal{H}_\infty$controllers. It is demonstrated, that the IROD method provides better overall closed loop system than the sequential design methods, by comparing the tracking performance, sensitivity, and control power. This example also shows that the IROD method is an effective alternative to existing integrated design methods and potential can offer better solutions than existing methods.

For the systems which can not be linearized at operating points, for example hydraulic actuators, but are feedback linearizable with minimum phase zero dynamics, feedback linearization provides best controllers. This method is known for not being robust to parameter variations. A new method for robust feedback linearization is proposed based on sensitivity dynamics for nonlinear systems with parametric uncertainties. For minimum phase systems, the stability of sensitivity augmented dynamics is proved. This method provides least conservative design because it does not require estimates of uncertainty bounds. A robust feedback linearized controller is designed using proposed method for hydraulic actuator with double acting cylinder and four way spool valve. The objective was to minimize the sensitivity of the closed loop system dynamics with respect to fluid density parameter. It is shown that augmenting control input using sensitivity information improves the robustness of the system.

The methodology explained in chapter 2 for lineairization of DAE in symbolic form can be extended to linearization of 3D multibody dynamics. The IROD methodology can be further extended to include parameter tolerance maximization and variability minimization problems. IROD has great potential if the linear system is parameter dependent. A parameter dependent Lyapunov function may be used to convert the optimal control problems into BMI constrained problems, and for a class of systems this non-convex problem may be converted into equivalent LMI constrained problem. IROD methodology can be extended to robust gain scheduling as well.

The robust feedback linearization method proposed here, can also be extended for back stepping control and adaptive control. While the methodology is demonstrated using SISO system example it readily extends to MIMO plant models with multiple uncertain parameters.

BIBLIOGRAPHY

[1] Bodden, D., and Junkins, J., 1985. "Eigenvalue optimization algorithms for structure/controller design iterations((for fflexible spacecraft))". *Journal of Guidance, Control, and Dynamics,* **8**, pp. 697–706.

[2] Onoda, J., and RT, H., 1987. "An approach to structure/control simultaneous optimization for large flexible spacecraft". *AIAA,* **25**, pp. 1133–1138.

[3] Padula, S., Sandridge, C., Walsh, J., and Haftka, R., 1992. "Integrated controls-structures optimization of a large space structure". *Computers and Structures,* **42**(5), pp. 725 – 732.

[4] Zeiler, T., and Gilbert, M., 1993. "Integrated control/structure optimization by multilevel decomposition". *Structural and Multidisciplinary Optimization,* **6**(2), pp. 99–107.

[5] Khot, N., 1995. "Optimum structural design and robust active control using singular value constraints". *Computational mechanics,* **16**(3), pp. 208–215.

[6] Tsujioka, K., Kajiwara, I., and Nagamatsu, A., 1996. "Integrated optimum design of structure and h control system". *AIAA journal,* **34**(1), pp. 159–165.

[7] Khot, N., and Öz, H., 1998. "Structral–control optimization with h2-and h-norm bounds". *Optimal Control Applications and Methods,* **18**(4), pp. 297–311.

[8] Lu, J., and Skelton, R., 2000. "Integrating structure and control design to achieve mixed h2/h performance". *International Journal of Control,* **73**(16), pp. 1449–1462.

[9] Bozca, M., Muğan, A., and Temeltaş, H., 2008. "Decoupled approach to integrated optimum design of structures and robust control systems". *Structural and Multidisciplinary Optimization,* **36**(2), pp. 169–191.

[10] Fu, K., and Mills, J., 2005. "A convex approach solving simultaneous mechanical structure and control system design problems with multiple closed-loop performance specifications". *Journal of dynamic systems, measurement, and control,* **127**(1), pp. 57–68.

[11] Pil, A., and Asada, H., 1996. "Integrated structure/control design of mechatronic systems using a recursive experimental optimization method". *Mechatronics, IEEE/ASME Transactions on,* **1**(3), sept., pp. 191 –203.

[12] Wu, F., Zhang, W., Li, Q., and Ouyang, P., 2002. "Integrated design and pd control of high-speed closed-loop mechanisms". *Transactions of the ASME,* **124**.

[13] Krishnaswami, P., and Kelkar, A., 2003. "Optimal design of controlled multibody dynamic systems for performance, robustness and tolerancing". *Engineering with Computers,* **19**, pp. 26–34. 10.1007/s00366-002-0246-.

[14] Carrigan, J., Kelkar, A., and Krishnaswami, P., 2005. "Integrated design and minimum sensitivity design of controlled multibody systems". *ASME Conference Proceedings,* **2005**(47438), pp. 601–609.

[15] Bode, H., 1952. *Network Analysis and Feedback Amplifier Design.* No. v. 8 in Bell Telephone Laboratories series. Van Nostrand.

[16] Horowitz, I., 1963. *Synthesis of Feedback Systems.* Academic Press.

[17] Tomović, R., 1963. *Sensitivity Analysis of Dynamic Systems.* McGraw-Hill electronic sciences series. McGraw-Hill.

[18] Bradt, A., 1968. "Sensitivity functions in the design of optimal controllers". *Automatic Control, IEEE Transactions on,* **13**(1), feb, pp. 110 – 111.

[19] Sobral, M., J., 1968. "Sensitivity in optimal control systems". *Proceedings of the IEEE,* **56**(10), oct., pp. 1644 – 1652.

[20] Sannuti, P., Cruz, J., Lee, I., and Bradt, A., 1968. "A note on trajectory sensitivity of optimal control systems". *Automatic Control, IEEE Transactions on,* **13**(1), feb, pp. 111 – 113.

[21] Eslami, M., 1994. *Theory of Sensitivity in Dynamic Systems: An Introduction.* Springer-Verlag.

[22] Fleming, P., 1973. *Trajectory Sensitivity Reduction in the Optimal Linear Regulator.* The Queen's University of Belfast.

[23] Fleming, P., and Newmann, M., 1977. "Design algorithms for a sensitivity constrained suboptimal regulator". *International Journal of Control,* **25**(6), pp. 965–978.

[24] Frank, P., 1978. *Introduction to System Sensitivity Theory.* Academic Press.

[25] Yedavalli, K., and Skelton, R., 1982. "Controller design for parameter sensitivity reduction in linear regulators.". *OPTIMAL CONTR. APPLIC. & METHODS.,* **3**(3), pp. 221–240.

[26] Youla, D., Jabr, H., and Bongiorno, J., J., 1976. "Modern wiener-hopf design of optimal controllers–part ii: The multivariable case". *Automatic Control, IEEE Transactions on,* **21**(3), jun, pp. 319 – 338.

[27] Zames, G., and Francis, B., 1983. "Feedback, minimax sensitivity, and optimal robustness". *Automatic Control, IEEE Transactions on,* **28**(5), pp. 585–601.

[28] Tulpule, P., and Kelkar, A., 2012. "Robust optimal control design using sensitivity dynamics and youla parameterization". In ASME DSCC/MOVIC Conference Proceedings, Fort Lauderdale FL, ASME.

[29] Boyd, S., El Ghaoui, L., Feron, E., and Balakrishnan, V., 1994. *Linear Matrix Inequalities in System and Control Theory*, Vol. 15. Society for Industrial Mathematics.

[30] El Ghaoui, L., and Niculescu, S., 2000. *Advances in Linear Matrix Inequality Methods in Control*, Vol. 2. Society for Industrial Mathematics.

[31] Scherer, C., Gahinet, P., and Chilali, M., 1997. "Multiobjective output-feedback control via lmi optimization". *Automatic Control, IEEE Transactions on,* **42**(7), pp. 896–911.

[32] Iwasaki, T., and Skelton, R., 1994. "All controllers for the general [infinity] control problem: Lmi existence conditions and state space formulas". *Automatica,* **30**(8), pp. 1307–1317.

[33] Pipeleers, G., Demeulenaere, B., Swevers, J., and Vandenberghe, L., 2009. "Extended lmi characterizations for stability and performance of linear systems". *Systems & Control Letters,* **58**(7), pp. 510–518.

[34] Tuan, H., and Apkarian, P., 2000. "Low nonconvexity-rank bilinear matrix inequalities: Algorithms and applications in robust controller and structure designs". *Automatic Control, IEEE Transactions on,* **45**(11), pp. 2111–2117.

[35] Goh, K., Safonov, M., and Papavassilopoulos, G., 1995. "Global optimization for the biaffine matrix inequality problem". *Journal of global optimization,* **7**(4), pp. 365–380.

[36] VanAntwerp, J. G., Braatz, R. D., and Sahinidis, N. V., 1997. "Globally optimal robust control for systems with time-varying nonlinear perturbations". *Computers & chemical engineering,* **21**, pp. S125–S130.

[37] El Ghaoui, L., Oustry, F., and AitRami, M., 1997. "A cone complementarity linearization algorithm for static output-feedback and related problems". *Automatic Control, IEEE Transactions on,* **42**(8), pp. 1171–1176.

[38] Kanev, S., Scherer, C., Verhaegen, M., and De Schutter, B., 2004. "Robust output-feedback controller design via local bmi optimization". *Automatica,* **40**(7), pp. 1115–1127.

[39] Yim, S., and Park, Y., 2011. "Design of rollover prevention controller with linear matrix inequality-based trajectory sensitivity minimisation". *Vehicle System Dynamics,* **49**(8), pp. 1225–1244.

[40] Tulpule, P., and Kelkar, A., 2013. "Bmi based robust optimal control synthesis via sensitivity minimization". In ASME - DSCC/MOVIC, Stanford University, Palo Alto, CA, ASME.

[41] Sohoni, V., and Whitesell, J., 1986. "Automatic linearization of constrained dynamical models". *Journal of Mechanisms, Transmissions and Automation in Design,* **108**(3), pp. 300–304.

[42] Liang, C., 1985. *Dynamic Analysis and Control Synthesis of Integrated Mechanical Systems.* University of Iowa.

[43] Kunkel, P., and Mehrmann, V. L., 2006. *Differential-algebraic equations: analysis and numerical solution.* European Mathematical Society.

[44] Shabana, A. A., 2013. *Dynamics of multibody systems.* Cambridge university press.

[45] Negrut, D., and Ortiz, J. L., 2006. "A practical approach for the linearization of the constrained multibody dynamics equations". *Journal of computational and nonlinear dynamics,* **1**(3), pp. 230–239.

[46] Ge, X.-S., Zhao, W.-J., Chen, L.-Q., and Liu, Y.-Z., 2005. "Symbolic linearization of differential/algebraic equations based on cartesian coordinates". *TECHNISCHE MECHANIK,* **25**(3-4), pp. 230–240.

[47] Xie, Y., Alleyne, A., Greer, A., and Deneault, D., 2011. "Fundamental limits in combine harvester header height control". In American Control Conference (ACC), 2011, IEEE, pp. 5279–5285.

[48] Xie, Y., and Alleyne, A., 2012. "Two degree of freedom controller on combine harvester header height control". In ASME - DSCC/MOVIC, Fort Lauderdale, ASME.

[49] Xie, Y., and Alleyne, A., 2011. "Integrated plant and controller design of a combine harvester system". In ASME - DSCC, Arlington, VA, USA, ASME.

[50] Stentz, A., Bares, J., Singh, S., and Rowe, P., 1999. "A robotic excavator for autonomous truck loading". *Autonomous Robots,* **7**(2), pp. 175–186.

[51] Singh, S., 1997. "State of the art in automation of earthmoving". *Journal of Aerospace Engineering,* **10**(4), pp. 179–188.

[52] Jun, Y., Bo, L., Yonghua, Z., and Haibo, Q., 2013. "A review on modeling, identification and servo control of robotic excavator". *International Journal of Engineering, Science and Technology,* **5**(4), pp. 14–22.

[53] Fales, R., and Kelkar, A., 2009. "Robust control design for a wheel loader using and feedback linearization based methods". {*ISA*} *Transactions,* **48**(3), pp. 312 – 320.

[54] Carrigan, J., 2003. "General methodology for multi-objective optimal design of control-structure nonlinear mechanisms with symbolic computing". Master's thesis, Iowa State University.

[55] Isidori, A., 1995. *Nonlinear control systems*, Vol. 1. Springer.

[56] Khalil, H. K., and Grizzle, J., 2002. *Nonlinear systems*, Vol. 3. Prentice hall Upper Saddle River.

[57] Hauser, J., Sastry, S., and Meyer, G., 1992. "Nonlinear control design for slightly non-minimum phase systems: Application to v/stol aircraft". *Automatica,* **28**(4), pp. 665 – 679.

[58] Spong, M. W., Thorp, J. S., and Kleinwaks, J. M., 1984. "The control of robot manipulators with bounded input: Part ii: Robustness and disturbance rejection". In Decision and Control, 1984. The 23rd IEEE Conference on, Vol. 23, IEEE, pp. 1047–1052.

[59] Spong, M. W., 1987. "Modeling and control of elastic joint robots". *Journal of dynamic systems, measurement, and control,* **109**(4), pp. 310–318.

[60] Freidovich, L. B., and Khalil, H. K., 2006. "Robust feedback linearization using extended high-gain observers". In Decision and Control, 2006 45th IEEE Conference on, IEEE, pp. 983–988.

[61] Elmali, H., and Olgac, N., 1992. "Robust output tracking control of nonlinear {MIMO} systems via sliding mode technique". *Automatica,* **28**(1), pp. 145 – 151.

[62] Levant, A., 2003. "Higher-order sliding modes, differentiation and output-feedback control". *International Journal of control,* **76**(9-10), pp. 924–941.

[63] Ioannou, P. A., and Sun, J., 2012. *Robust adaptive control*. Courier Dover Publications.

[64] Piltan, F., Rezaie, H., Boroom, B., and Jahed, A., 2012. "Design robust backstepping on-line tuning feedback linearization control applied to ic engine". *International Journal of Advance Science and Technology,* **42**, pp. 183–204.

[65] Talole, S., and Phadke, S., 2009. "Robust inputoutput linearisation using uncertainty and disturbance estimation". *International Journal of Control,* **82**(10), pp. 1794–1803.

[66] Zhang, R., Prasetiawan, E., and Alleyne, A., 2002. "Modeling and h2/h mimo control of an earthmoving vehicle powertrain". *Journal of dynamic systems, measurement, and control,* **124**(4), pp. 625–636.

[67] Li, G., and Khajepour, A., 2005. "Robust control of a hydraulically driven flexible arm using backstepping technique". *Journal of Sound and Vibration,* **280**(3), pp. 759–775.

[68] Nakkarat, P., and Kuntanapreeda, S., 2009. "Observer-based backstepping force control of an electrohydraulic actuator". *Control Engineering Practice,* **17**(8), pp. 895–902.

[69] Alleyne, A. G., and Liu, R., 2000. "Systematic control of a class of nonlinear systems with application to electrohydraulic cylinder pressure control". *Control Systems Technology, IEEE Transactions on,* **8**(4), pp. 623–634.

[70] Jelali, M., and Kroll, A., 2003. *Hydraulic servo-systems: modelling, identification and control*. Springer.

[71] Yao, B., Bu, F., and Chiu, G. T., 2001. "Non-linear adaptive robust control of electro-hydraulic systems driven by double-rod actuators". *International Journal of Control,* **74**(8), pp. 761–775.

[72] Nikravesh, P. E., 2007. *Planar Multibody Dynamics: Formulation, Programming and Applications*. CRC Press, Inc.

[73] Clairaut, A., 1734. *Histoire Acad. R. Sci. Paris*.

[74] Niksefat, N., and Sepehri, N., 2001. "Designing robust force control of hydraulic actuators despite system and environmental uncertainties". *Control Systems, IEEE,* **21**(2), Apr, pp. 66–77.